

19941228 074

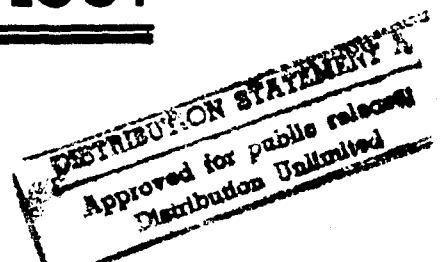
EXPERIMENTAL INVESTIGATION OF THE
EFFECTS OF RELATIVE PHYSICAL
ORIENTATION BETWEEN EVAPORATOR
AND CONDENSER FOR A LOOP HEAT PIPE

THESIS

Brad R. Thompson, Captain, USAF

DEPARTMENT OF THE AIR FORCE
AIR UNIVERSITY
AIR FORCE INSTITUTE OF TECHNOLOGY

Wright-Patterson Air Force Base, Ohio



AFIT/GA/ENY/94D-10

EXPERIMENTAL INVESTIGATION OF THE
EFFECTS OF RELATIVE PHYSICAL
ORIENTATION BETWEEN EVAPORATOR
AND CONDENSER FOR A LOOP HEAT PIPE

THESIS

Brad R. Thompson, Captain, USAF

AFIT/GA/ENY/94D-10

DTIC QUALITY INSPECTED 2

Approved for public release; distribution unlimited

AFIT/GA/ENY/94D-10

EXPERIMENTAL INVESTIGATION OF THE EFFECTS OF RELATIVE
PHYSICAL ORIENTATION BETWEEN EVAPORATOR AND
CONDENSER FOR A LOOP HEAT PIPE

THESIS

Presented to the Faculty of the School of Engineering
of the Air Force Institute of Technology
Air University
In Partial Fulfillment of the
Requirements for the Degree of
Master of Science in Astronautical Engineering

Brad R. Thompson, B.S.E.

Captain, USAF

December 1994

Accession For	
NTIS GRA&I	<input checked="" type="checkbox"/>
DTIC TAB	<input type="checkbox"/>
Unannounced	<input type="checkbox"/>
Justification	
By	
Distribution/	
Availability Codes	
Dist	Avail and/or Special
A-1	

Approved for public release; distribution unlimited

Preface

Heat pipes have been an area of interest to me long before I took my first class in Thermodynamics, where I started to gain an appreciation for how they work. This Thesis has provided me a chance to work with the latest developments in heat pipe technology, the loop heat pipe. I have enjoyed the opportunity to put one of these new devices to the test. Hopefully, the results found here will provide useful information for the future designers of these new devices.

There have been several people who have helped make this research possible. First I would like to thank Lt Col Bowman, my thesis advisor, for encouraging me to pursue an area of interest and pointing me to the people who could make things happen. This brings me to Dr. Jerry Beam, whom I would like to thank for allowing me the opportunity to work in the lab he oversees and for entrusting me with one of the few Russian heat pipes in the United States. Additionally, I would like to thank Don Reinmuller, John Leland, John Tennant, and Don Brightner for the day to day assistance they provided me in getting the pipe instrumented and the test equipment up and running. A special note of thanks is due to Gary Grogg who assisted me during much of the actual testing.

Finally, I want to thank my wife Lisa and sons Brett and Alex for the love and support they have shown me throughout this effort.

Brad R. Thompson

Table of Contents

	Page
Preface	ii
List of Figures	vii
List of Tables	ix
Abstract	x
I. Introduction	1-1
A. Thesis	1-1
B. Background	1-1
C. Justification	1-4
D. Thesis Contents	1-5
II. Approach	2-1
A. Introduction	2-1
B. Experimental Set-up	2-1
1. Description of Pipe	2-1
2. Description of Pipe Layout	2-2
3. Instrumentation of the Pipe	2-2
4. Test Equipment and Data Acquisition Equipment	2-3
C. Tests Performed	2-5
1. Specific Configurations Tested	2-5
i. Varying Relative Angles	2-5
ii. Varying Relative Heights	2-7
iii. Varying Relative Heights and Angles	2-8
2. Heat Input	2-9
3. Coolant Temperatures	2-9

III. Data Description and Analysis	3-1
A. Evaluation Criteria	3-1
B. Data Description and Reduction	3-1
C. Uncertainty Analysis	3-3
IV. Discussion of Results	4-1
A. Discussion of Graphs	4-1
1. Comparison of Varying Evaporator Angles between 20 °C and 40 °C Coolant Inlet Temperatures at No Relative Height Difference	4-1
i. Varying Evaporator Angles at 40 °C Coolant Inlet Temperature	4-1
ii. Varying Evaporator Angles at 20 °C Coolant Inlet Temperature	4-3
2. Comparison Of Varying Condenser Angles between 20 °C and 40 °C Coolant Inlet Temperatures at No Relative Height Difference	4-4
i. Varying Condenser Angles at 20 °C Coolant Inlet Temperature	4-4
ii. Varying Condenser Angles at 40 °C Coolant Inlet Temperature	4-6
3. Comparison of Varying Evaporator Angles at Evaporator-Over-Condenser Height Differences of: 0 meters, 1.22 meters, and 2.44 meters	4-7
i. Varying Evaporator Angles at Evaporator-Over-Condenser Height Difference of 1.22 meters	4-8
ii. Varying Evaporator Angles at Evaporator-Over-Condenser Height Difference of 2.44 meters	4-8
4. Comparison of Varying Condenser Angles at Evaporator-Over-Condenser Height Differences of: 0 meters, 1.22 meters, and 2.44 meters	4-11
i. Varying Condenser Angles at Evaporator-Over-Condenser Height Differences of 1.22 meters	4-12
ii. Varying Condenser Angles at Evaporator-Over-Condenser Height Differences of 2.44 meters	4-14

iii. Performance Dependence on Condenser Angular Orientation	4-16
5. Comparison of Varying Relative Heights at Fixed Horizontal Angular Orientations	4-17
i. Evaporator-Over-Condenser Orientations	4-18
ii. Condenser-Over-Evaporator Orientations	4-18
6. Trends Attributable to Coolant Inlet Temperature	4-20
i. Summary of Comparison for Varying Evaporator Angles Between 20 °C and 40 °C Coolant Inlet Temperatures at No Relative Height Difference	4-20
ii. Summary for all Angular Orientations	4-21
B. Other Observations	4-21
1. Q_{in} Sensitivity	4-21
2. Observation of a ΔT Anomaly	4-21
3. Evaporator Angle Performance Enhancement	4-22
C. Performance Degradation	4-23
1. Observed Failure Modes	4-23
i. Sensitivity to Decreases in Input Power	4-23
ii. Minimum Q_{in} Dependence on Evaporator Angles.	4-23
2. Performance Degradation with ΔH	4-23
V. Conclusions and Recommendations	5-1
A. Conclusions:	5-1
1. Performance Dependence on Evaporator Angle	5-1
2. Performance Dependence on Condenser Angle	5-1
3. Performance Dependence on Coolant Temperature	5-2
4. Performance Dependence on Relative Heights of Evaporator Over Condenser	5-2
5. Q_{in} Influences	5-2
B. Recommendations:	5-3
1. Continue Evaluation of the Sensitivity to Step Decreases in Q_{in}	5-3
2. Evaluate Performance Dependence on Various Line Routings	5-3
3. Continue Evaluation of the ΔT Anomaly	5-3

Appendix A: Loop Heat Pipe (LHP) Operation	A-1
Appendix B: Sample of Data Recorded	B-1
Appendix C: Uncertainty Calculations	C-1
Appendix D: Test Matrix	D-1
Bibliography	BIB-1
Vita	

List of Figures

Figure		Page
1.1	Loop Heat Pipe	1-2
2.1	Line Routing of Loop Heat Pipe Test Set-up	2-1
2.2	Thermocouple Locations	2-3
2.3	Test Equipment Layout	2-4
2.4	No Relative Height, Varying Angular Orientations	2-7
2.5	Varying Relative Height, Fixed Horizontal Angular Orientation	2-7
2.6	Varying Evaporator Heights and Evaporator and Condenser Angular Orientations	2-8
4.1	Delta T vs Q_{in} , No Relative Height Differences, Varying Evaporator Angles, 40 °C Coolant Temperature	4-2
4.2	Delta T vs Q_{in} , No Relative Height Differences, Varying Evaporator Angles, 20 °C Coolant Temperature	4-3
4.3	Delta T vs Q_{in} , No Relative Height Differences, Varying Condenser Angles, 20 °C Coolant Temperature	4-5
4.4	Delta T vs Q_{in} , No Relative Height Differences, Varying Condenser Angles, 40 °C Coolant Temperature	4-7
4.5	Delta T vs Q_{in} , 1.22 meter Height Difference, Varying Evaporator Angles, 20 °C Coolant Temperature	4-9
4.6	Delta T vs Q_{in} , 2.44 meter Height Difference, Varying Evaporator Angles, 20 °C Coolant Temperature	4-10
4.7	Obstruction of Vapor Line	4-12

4.8	Delta T vs Q_{in} , 1.22 meter Height Difference, Varying Condenser Angles, 20 °C Coolant Temperature	4-14
4.9	Delta T vs Q_{in} , 2.44 meter Height Difference, Varying Condenser Angles, 20 °C Coolant Temperature	4-15
4.10	Delta T vs Q_{in} , Varying Evaporator over Condenser Heights, Evaporator and Condenser Horizontal, Coolant Temperature 20 °C	4-18
4.11	Delta T vs Q_{in} , Varying Condenser over Evaporator Heights, Evaporator and Condenser Horizontal, Coolant Temperature 20 °C	4-19

List of Tables

Table		Page
2.1	Equipment Used	2-6
4.1	Varying Evaporator Angles and Heights, Summary Data	4-13

ABSTRACT

This research examined the effects on performance of varying angular orientation and height differences between evaporator and condenser for a loop heat pipe. Performance was defined as the difference in temperature between evaporator and condenser (ΔT). The pipe was evaluated at varying input power (Q_{in}) for: varying evaporator and condenser angles, different coolant temperatures, and varying relative height differences. All analysis included only steady state operation. The performance was influenced by condenser angles, with an optimal condenser angle for best performance being +45 degrees from horizontal. Additionally, the evaporator angles were found to influence performance only at low Q_{in} and low coolant temperatures. For high Q_{in} , performance was independent of evaporator angle. For small Q_{in} the ΔT increased (poorer performance) with decreasing coolant temperature. However, for high Q_{in} the ΔT was independent of coolant temperature. For small Q_{in} , the ΔT increased with increasing heights of evaporator over condenser. However, for high Q_{in} the ΔT was independent of the height difference. Additionally, pipe operation was sensitive to the rate of decrease of Q_{in} . Finally, an unexplained anomaly shows the pipe to operate at two different ΔT values for a given heat input.

EXPERIMENTAL INVESTIGATION OF THE EFFECTS OF RELATIVE PHYSICAL ORIENTATION BETWEEN EVAPORATOR AND CONDENSER FOR A LOOP HEAT PIPE

I. Introduction

A. Thesis

This research experimentally investigates the effects on performance of relative physical orientations of the evaporator and condenser of a loop heat pipe (LHP). Relative physical orientations include angular displacements of the evaporator and condenser, and height differences between evaporator and condenser. The research objectives are: to map the performance of a loop heat pipe for relative evaporator and condenser elevations at varying relative angular orientations within a gravity field and; to determine possible failure modes of a loop heat pipe.

B. Background

A loop heat pipe is a heat transfer device which takes advantage of the heat of vaporization of a working fluid to generate vapor pressure to pump the working fluid. A loop heat pipe operates much the same as a standard heat pipe except that it is a pressure driven device instead of a capillary driven device (see Figure 1.1). A loop heat pipe has an evaporator end into which heat is input, vaporizing a working fluid. The vapor is then transferred to the opposite end of the pipe to the condenser, where heat is removed. The

vapor then condenses to a liquid which is returned to the evaporator section and the process continued.

The evaporator consists of a porous wick structure which uses capillary force to draw and deliver liquid to a surface which is exposed to a heat source. At the heat absorbing surface of the wick, there are integrated passage ways (point 8 of Figure 1.1) which allow vapor to be communicated to an exhaust port in the shell of the evaporator (point 2 of Figure 1.1). The vapor then passes through a vapor line to the condenser section. The condenser section is in communication with a heat sink where the vapor releases its thermal energy and condenses back to a liquid (point 4 of Figure 1.1). The liquid is then transported back to the evaporator through a liquid return line (point 5 of Figure 1.1). The liquid is forced through the liquid line to the wick in the evaporator by the vapor pressure (point 6 of Figure 1.1), where it can be drawn again through the wick.

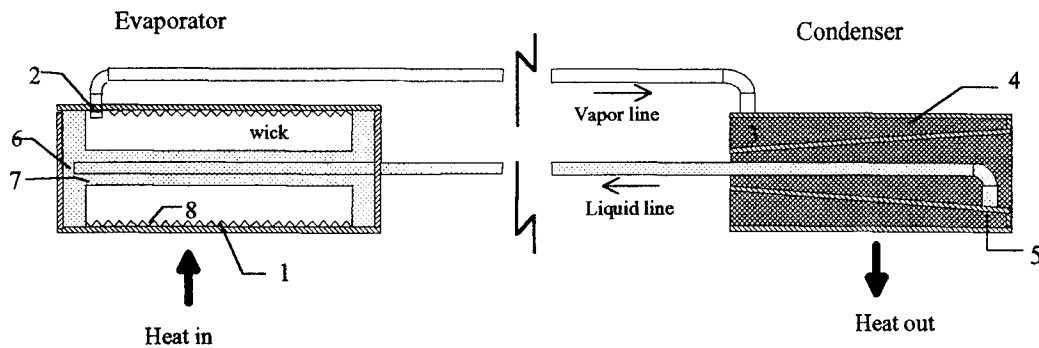


Figure 1.1 Loop Heat Pipe (Maidanik et al., 1985)

A more detailed explanation of the operation of a loop heat pipe is provided in Appendix A, and by Maidanik et al. in their US Patent Number 4,515,209.

The original loop heat pipe concept was invented in 1966 by American, F. J. Stenger (Maidanik, 1991). Recent developments in loop heat pipe technology have been accomplished almost exclusively in what was formerly known as the Soviet Union, with little expertise or knowledge of these devices within the United States Department of Defense (Beam, 1994). The loop heat pipe considered in the current study is of Soviet origin in both its design and manufacture.

Recent experimental research has examined the steady and transient operating characteristics of loop heat pipes with respect to gravity, that is, the LHP with the evaporator placed above the condenser (Dickey and Peterson, 1994; Meyer et al., 1993). A loop heat pipe, practically the same as that proposed here, was evaluated by Dickey and Peterson. The loop heat pipe they tested was made of stainless steel and was approximately three meters long with vapor and liquid lines of 4 mm and 3 mm outside diameter, respectively. The working fluid for their heat pipe was ammonia. Ammonia is the working fluid used in the current study. Dickey and Peterson positioned the evaporator at various heights above the condenser. However, the orientation of both the evaporator and condenser was allowed to rotate with the tilt angle of the pipe. No consideration was given to the relative angular orientation with respect to gravity, or angular orientation between evaporator and condenser. Dickey and Peterson's loop heat pipe was found to operate as long as the evaporator was less than 25.4 centimeters above the condenser. However, above 25.4 centimeters of relative height difference of evaporator over condenser, the loop heat pipe failed to start. Once the loop heat pipe was

operating, the relative height difference could be increased up to 61 centimeters before system failure.

To date, Dickey and Peterson have been the only ones to present an analytical model for loop heat pipe performance. Their model has low fidelity in that it only considers bulk temperatures of the liquid and vapor and the mass flow rates and makes no provisions for internal geometries. It is also restricted to only horizontal configurations (Dickey and Peterson, 1994). This horizontal restriction does not allow for the application of the model to the various angular orientations of the heat pipe tested here.

An additional loop heat pipe configuration has been evaluated by Meyer et al. The construction of their pipe is considerably different from the heat pipe tested in this effort. The performance of the Meyer et al. loop heat pipe was evaluated for different angular orientations with respect to gravity, but not for relative angular orientations between evaporator and condenser.

C. Justification

Loop heat pipes are being increasingly considered for thermal control applications in aircraft and spacecraft. To insure adequate design of the thermal control system for the aircraft or spacecraft it is important to understand the performance of a given heat pipe design. Additionally, it must be understood what the potential failure modes are, or the conditions under which performance degradation can be expected.

Due to the physical layout of the loop heat pipe to be tested, there was a question as to how it would perform at certain angular orientations. It was suspected the heat pipe

would not perform when the condenser was oriented such that the inlet to the liquid return line was in the vertical direction (see Figure 1.1). Due to this construction, it was believed that at certain angular orientations, the performance of the loop heat pipe would begin to degrade. As mentioned in the research objectives, it is desired to determine what those limited performance orientations are and to quantify any performance degradation.

As part of the purchase of the given loop heat pipe by Wright Laboratory, Thermacore, the facilitator, provided initial test data. The data showed that testing was accomplished for various angular orientations and relative heights between the evaporator and condenser. The data indicates there is performance degradation, however, the data is insufficient to quantify the extent of this degradation (Russian Loop Heat Pipe, 1992). The test set-up used to gather the data was done as a quick preliminary look. No attempt was made to control extraneous environmental influences on the LHP performance, i.e. the heater input to the evaporator was uninsulated, thus the amount of energy input to the pipe was unknown.

In summary, little experimental or analytical work has been done on the effects of relative angular orientations of the evaporator to the condenser for various height differences in a gravity field. An understanding of the potential effects is necessary if these loop heat pipes are to be effectively employed.

D. Thesis Contents

Chapter One of this thesis contains an introduction to loop heat pipes and the specific problem to be evaluated. Chapter Two presents the approach taken to evaluate

the problem. Chapter Three describes the data and its analysis. Chapter Four presents a discussion of the results and finally Chapter Five presents conclusions and recommendations.

II. Approach

A. Introduction

This section will describe the experimental set up and present the various tests used to evaluate the loop heat pipe performance.

B. Experimental Set-up

1. Description of Pipe. The loop heat pipe tested was known to have ammonia as the working fluid with a stainless steel enclosure (Beam, 1994). The wick structure material is unknown. The evaporator heat input section was 1.2 cm in diameter and was mounted in an 8.0 cm by 3.0 cm by 1.8 cm block. The evaporator reservoir section on the outside end was 1.2 cm in diameter by 9.4 cm long and on the inside end was 1.9 cm in diameter by 9.4 cm long (see Figure 2.1). The condenser heat removal section was 1.2 cm

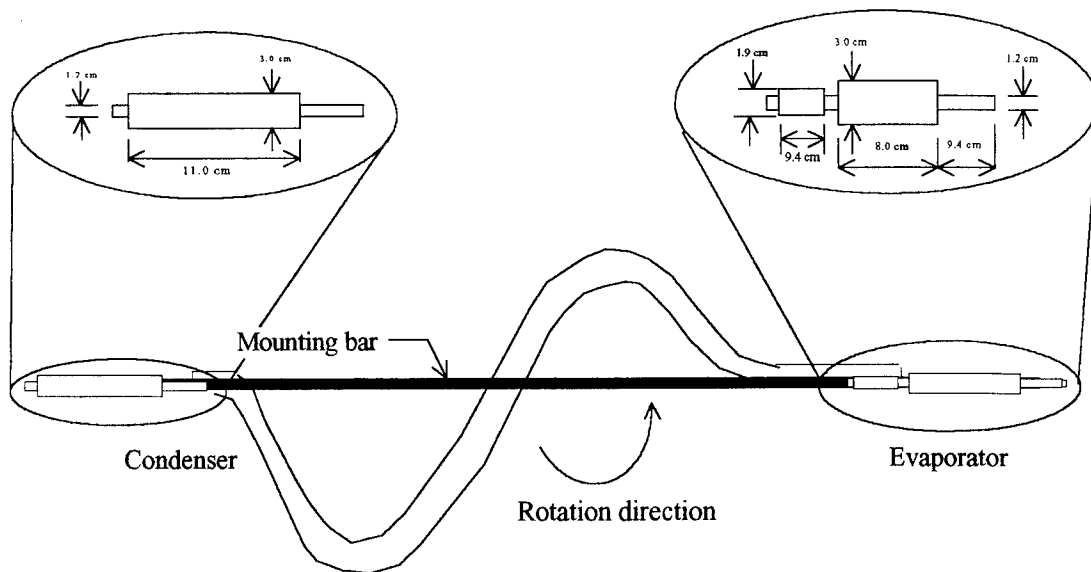


Figure 2.1 Loop Heat Pipe Test Set-up

in diameter and was mounted in an 11.0 cm by 3.0 cm by 1.8 cm block. The vapor and liquid lines were both 3.0 millimeters outside diameter and 3.48 meters long.

2. Description of Pipe Layout. The heat pipe was mounted on a 3.05 meter bar which was allowed to rotate about a rotation axis perpendicular to the page of Figure 2.1. Since the bar was shorter than the length of the heat pipe, the length of the vapor and liquid lines were arranged such that they formed a large 'S' shape (see Figure 2.1).

Throughout the testing, the arrangement of the lines varied to allow positioning at the desired evaporator and condenser angular orientations. The evaporator and the condenser were mounted on plates, which allowed their independent rotation of ± 90 degrees with respect to the axis of the mounting bar. These plates facilitated all desired relative angular orientations between evaporator and condenser for all mounting bar positions.

3. Instrumentation of the Pipe. The pipe was instrumented with copper constantan 30 SWG nylon insulated thermocouples throughout. Along the evaporator end of the pipe, two thermocouples were mounted to the end reservoir, three to the actual evaporator section, one to the adiabatic section, and two to the inside end reservoir (see Figure 2.2). The center thermocouple on the heat input section of the evaporator was used to provide input to the safety controller. At 13 locations along the liquid and vapor lines, adjacent pairs of thermocouples were mounted, one thermocouple on the vapor line and one on the liquid line. At the condenser end, five thermocouples were placed for temperature measurements.

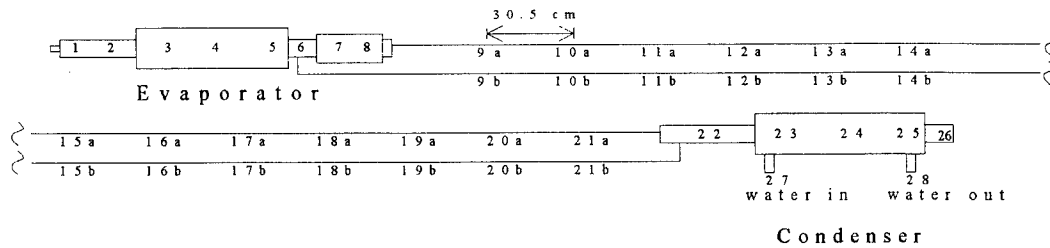


Figure 2.2 Thermocouple Locations

The pipe was insulated throughout with 1.27 cm thick black foam pad. An additional thermocouple was mounted on the exterior of the foam insulation at the evaporator. All thermocouples, except for the safety controller thermocouple, were input to a Fluke data logger for data acquisition.

4. Test Equipment and Data Acquisition Equipment. Heat input to the evaporator was supplied with electrical resistance heating. The amount of input power was determined from the value of the heaters resistance and the measured current flowing through it. To supply power to the heater, a Sorensen model number DCR 600-1.5B, 0-600 V, 0-3 Amp power supply was used. The layout of the equipment is shown in Figure 2.3. A summary of the equipment used is found in Table 2.1.

To measure the current and the power going to the heater, a Magtrol Power Analyzer, model 4612B power meter was used. The DC current to the evaporator heater was run through the power meter. This meter was used as a quality check to compare with the values measured by the Fluke data logger.

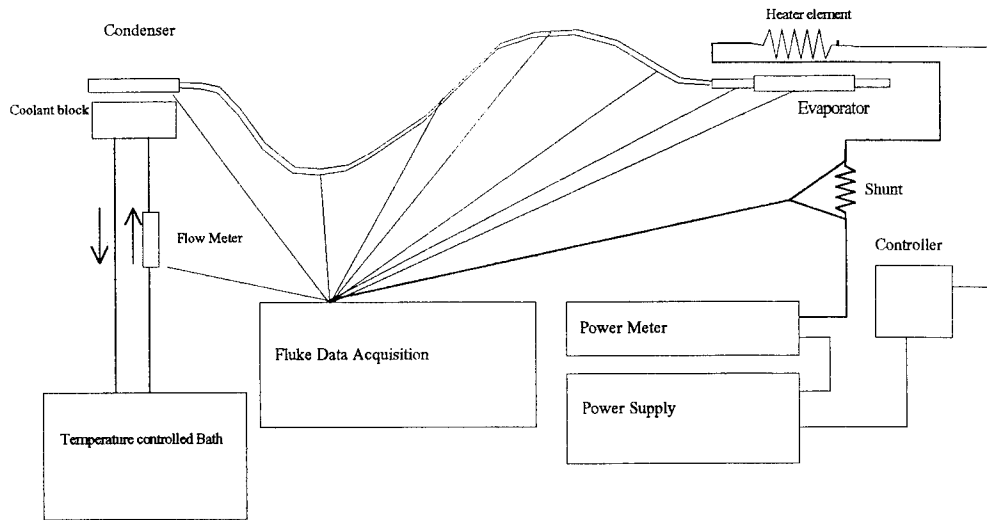


Figure 2.3 Test Equipment Layout

A precision resistor shunt was used as a means of measuring the current, which could then be recorded in the data logger. The current was used with the known heater resistance to determine the input power to the evaporator.

The Fluke data logger was the central component of the data acquisition system. The logger was programmed to scan all input channels every two minutes. The channels included all thermocouples and voltage measurements. The voltage measurements taken were those used to determine the current through the heater (the voltage across the shunt) and the voltage provided by the flowmeter circuitry, which indicated coolant flow rate at the condenser. Additional data items logged were: the ambient temperatures, and the coolant input and output temperatures. The data logger accomplished all necessary calculations, determining thermocouple temperatures and unit conversions required for finding input and output power. Additionally, the data logger was programmed to determine the steady state operating condition of the pipe (by checking if the average

condenser temperature had changed by less than 0.15 °C over a two minute interval).

Once a steady state was attained, the data logger saved all data points to disk upon each scan.

A controller was set up to ensure the pipe did not exceed a 60 °C maximum operating temperature, set to prevent rupture of the pipe. To prevent exceeding the temperature limit, the controller monitored the center thermocouple on the evaporator. When the controller detected the temperature was above the limit it shut off input power to the evaporator heater.

A flow meter, along with input and output thermocouples immersed in the coolant flow, determined the heat output at the condenser. The heat output at the condenser was used as a check to determine if the pipe was operating.

C. Tests Performed

In all, 48 tests were performed. The first two tests were used to insure all testing and data acquisition equipment were functioning properly. The remaining tests and their configurations are given in what follows. A complete listing of the tests and the various orientations is included in Appendix D.

1. Specific Configurations Tested. To determine the loop heat pipe performance, tests were run at varying relative evaporator and condenser angles, and at varying relative heights of evaporator-over-condenser, and condenser-over-evaporator.

i. Varying Relative Angles. With the evaporator and condenser at the same relative height, the angle of the evaporator was varied keeping the condenser horizontal.

Table 2.1 Equipment Used

Equipment	Manufacturer	Model number	Accuracy
Data Acquisition	Fluke	2286 Data Logging System	Temperature: ± 0.65 °C Voltage: range: 64mV; 0.01% + 8.0 μ V range: 512mV; 0.01% + 40 μ V range: 8V; 0.01% + 800 μ V range: 64V; 0.02% + 4mV
Power Analyzer	Megtrol	4612B	0.2% of reading or 0.25% of full scale
Power Supply	Sorensen	DCR 600-1.5B	Voltage: 0.1% Current: 0.25%
Controller	Honeywell	DC 3003-0-00B-2-0 0-0111	0.20% full scale (temperature °C)
Refrigerated and Heated coolant	Forma Scientific	2095	at 20 °C ± 1 °C
Flow meter	Omega	FTB 601	$\pm 1\%$ of reading
Shunt			1%
Heater	Minco	HK 14942 (-) DC 9038/9405	± 1 Ω at 23°C

Then the angle of the condenser was varied keeping the evaporator horizontal (see Figure 2.4). The angles evaluated included +135, +90, +45, 0, -45, and -90 degrees, for the evaporator and +90, +45, 0, -45, and -90 degrees for the condenser. The heat input block of the evaporator and the heat rejection block of the condenser were used for measuring the angles. These tests were included to determine the influence of relative angular orientation of the evaporator (and condenser) with respect to a gravity field. Ideally it was

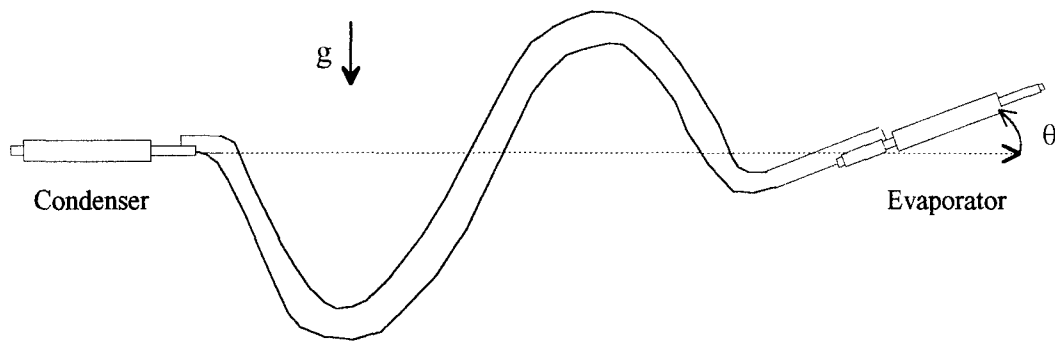


Figure 2.4. No Relative Height, Varying Angular Orientations

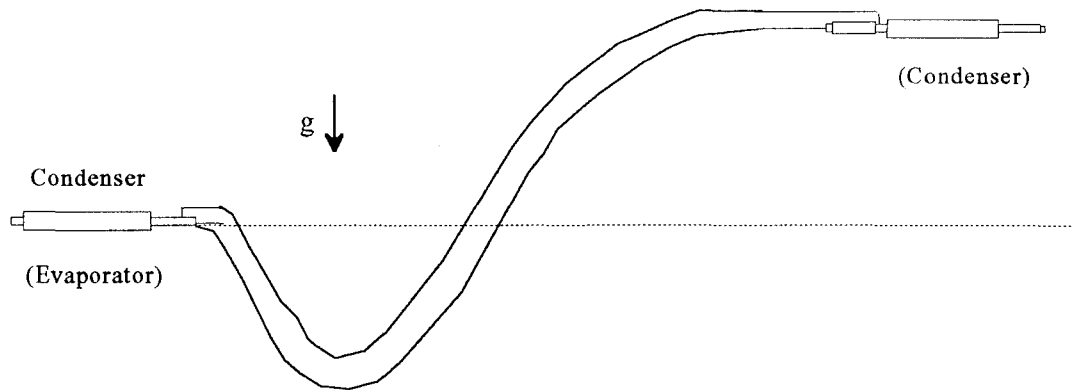


Figure 2.5. Varying Relative Height, Fixed Horizontal Angular Orientation

intended to provide insight into the magnitude of the effects of angular orientation only, since the evaporator and condenser were at the same relative height.

ii. Varying Relative Heights. In order to determine the performance of the loop heat pipe for relative height differences, the evaporator and condenser angles were fixed to zero degrees relative to horizontal, and the height of the evaporator over the condenser was varied, as well as the condenser height over the evaporator (see Figure

2.5). The height differences the loop heat pipe was evaluated at included: 0, 0.61, 1.22, 1.83, 2.44, and 2.79 meters.

iii. Varying Relative Heights and Angles. With the evaporator above the condenser, the angle of the evaporator was varied while fixing the condenser angle at a horizontal position (see Figure 2.6). The angles evaluated were again: +90, +45, 0, -45, and -90 degrees. The heights of the evaporator over the condenser that these test were run at included: 0, 1.22, and 2.44 meters. These tests were to provide insight into the influence of the evaporator heights and angular orientation on performance.

For the same evaporator-over-condenser heights, the evaporator was fixed at the horizontal position and the condenser angle allowed to vary (see Figure 2.6). The angles evaluated were again: +90, +45, 0, -45, and -90 degrees. This series of tests was to provide insight into the influence of the condenser orientation on performance.

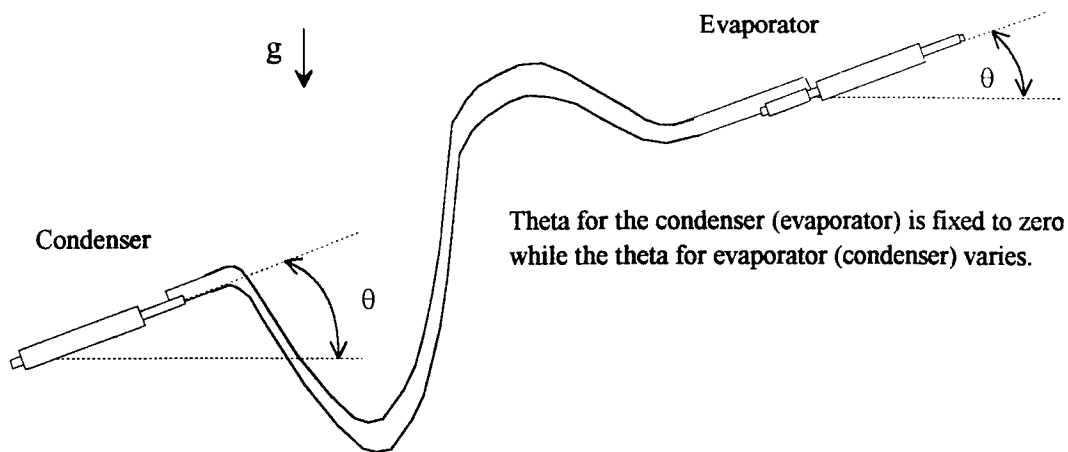


Figure 2.6

Varying Evaporator Heights and Evaporator and Condenser Angular Orientations

2. Heat Input. The envelope of heat inputs for the tests ranged from a typical low of 15 watts to a high of up to 125 watts. A low of 15 watts was attempted for all test. Some testing was accomplished in which heat inputs as low as 3 watts were attained. The upper heat input setting was determined by the evaporator temperature, where the evaporator temperature was kept below 60 °C to prevent pipe rupture.

3. Coolant Temperatures. For the initial tests, with no relative height difference between the evaporator and condenser (Figure 2.4), the tests were run with the coolant inlet temperature set at 20 °C and 40 °C. The remaining test configurations were run only at a 20 °C coolant temperature. These two temperatures were chosen to represent temperatures which may be experienced on an aircraft. The 20 °C coolant temperature was used for the majority of the tests since the coolant bath equipment easily maintained this temperature, whereas the 40 °C coolant temperature required additional manually controlled heaters. The coolant flow rate was set between 0.1 to 0.2 liters per minute. No attempt was made to control the condenser temperature.

III. Data Description and Analysis

This section presents the criteria used for evaluating the loop heat pipe's performance, and defines the data reduction accomplished to develop the graphs used for evaluating the performance. The section ends with a discussion of the uncertainty analysis.

A. Evaluation Criteria

One measure of a heat pipes performance is the difference in temperature (ΔT), between the evaporator and the condenser, required to maintain the transfer of heat energy. The smaller the temperature difference for a given energy throughput, the better the heat pipe performance. This temperature difference was used as the primary indicator of heat pipe performance.

The ΔT is plotted against the heat input at the evaporator (Q_{in}). The heat input to the evaporator is used since its value is known more accurately than the heat output. As such, analysing the ΔT as a function of Q_{in} will provide an indication of the loop heat pipe's ability to transfer heat energy away from a source.

B. Data Description and Reduction

Data was recorded from all thermocouples mounted on the pipe. However, for the analysis, only the heat input to the evaporator and the temperature of the evaporator and condenser were used. Q_{in} was determined by measuring the voltage across a shunt resistor

in series with the evaporator heater. Knowing the shunt resistance, voltage across it, and the resistance of the heater, the power, Q_{in} , was calculated. It is assumed that the majority of the heat input is delivered to the evaporator. Appendix C calculates the estimate of the Q_{in} to the evaporator which is convected away. The maximum amount found to be convected away at the evaporator was less than 1.2 watts. The pipe was equipped to monitor heat out flow at the condenser. A heat balance was accomplished on the pipe by measuring the heat taken out at the condenser. This was done by measuring the flow rate of the coolant to the coolant block and measuring the inlet and exit temperatures of the coolant. The heat removed from the coolant block was calculated using the specific heat of the coolant, the coolant flow rate, and the difference between coolant inlet and exit temperatures. For the majority of the tests the heat removed was within the experimental uncertainty of the measurements. For the tests where the heat removed was not within the experimental uncertainty the loss was attributed to parasitic losses through the insulation.

The definition of a data point used for analysis is the steady state ΔT vs Q_{in} . To determine the ΔT for each data point, the two thermocouple temperatures on the evaporator were averaged as well as the three thermocouple temperatures on the condenser and the difference between them used as the ΔT . To determine when the pipe was at steady state the average condenser temperature was used. Steady state was defined to be less than a 0.15 °C temperature change over a two minute interval while maintaining the heat input at a constant value. These data were taken for a total of 46 tests for various relative angular and height orientations.

To reduce the data for plotting, the data was reviewed and all non steady state data points removed. Then, at each heat input setting, the steady state points were averaged. With the exception of the first ten tests, data was taken to insure at least five steady state points at each heat input setting were recorded for averaging. After the tenth test it was decided that to ensure a steady state condition, additional settling time would be provided. A sample of the data recorded is included as Appendix B. The data was reduced to produce graphs of ΔT vs Q_{in} . These graphs were then combined with one another to compare the effects of angular orientation of evaporator and condenser and to assess the effect of angular orientation in combination with height differences.

C. Uncertainty Analysis

The uncertainty in the ΔT is fixed for all data taken and was determined to be ± 1.30 °C. The uncertainty for Q_{in} is approximately 5.0% of the input setting (see Appendix C for uncertainty calculations).

IV. Discussion of Results

This chapter will focus on the results of the testing accomplished. It begins by comparing the influences of coolant inlet temperature, angular orientations, and the height differential between components on the performance of the LHP. The chapter goes on to relate other items of interest observed during the testing, and finally concludes with a presentation of the factors which contribute to performance degradation.

A. Discussion of Graphs

Much of the comparative analysis between tests is related in terms of the negative or positive slope of the ΔT vs. Q_{in} graphs. As mentioned in Chapter Three, the ΔT is a measure of the LHP's performance. Therefore, knowledge of how the ΔT is influenced by coolant inlet temperatures, angular orientations, and height differences is of interest.

The balance of this thesis will compare the ΔT vs Q_{in} graphs at the various orientations. The figures are arranged to first present the varying evaporator and condenser angle effects at the various heights, which account for eight sets of graphs. The remaining two sets of graphs present the effects of varying heights at fixed horizontal angles.

1. Comparison of Varying Evaporator Angles for 20 °C and 40 °C Coolant Inlet Temperatures at No Relative Height Difference. In this section the effects on performance of coolant inlet temperature and evaporator angles will be discussed.

i. Varying Evaporator Angles at 40 °C Coolant Inlet Temperature.

Figure 4.1 contains the varying evaporator angle graphs for the 40 °C coolant inlet

temperature where there is no relative height difference between evaporator and condenser. The graphs in Figure 4.1 indicate that the LHP operates only in a positive slope range for all angular orientations and heat inputs. This trend of increasing ΔT with increasing heat input is what would be expected for a conventional heat pipe. The tight grouping of the graphs appear to indicate there is no evaporator angular dependence on

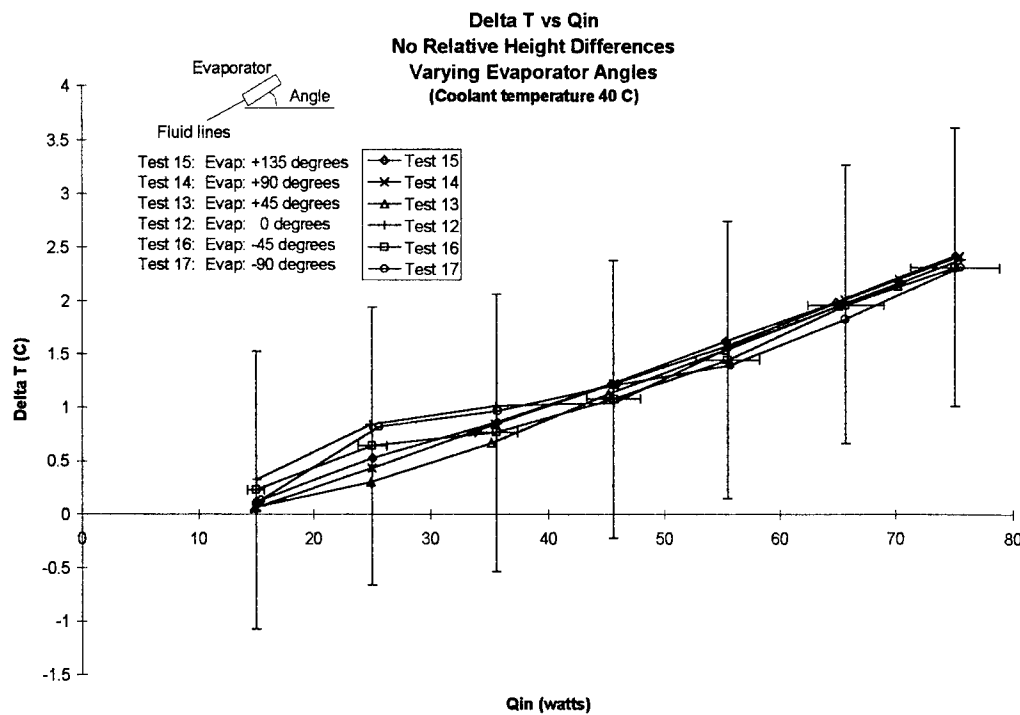


Figure 4.1 Delta T vs Q_{in} , No Relative Height Differences, Varying Evaporator Angles, 40 °C Coolant Temperature

performance at the 40 °C coolant inlet temperature. It was also noted that for all evaporator angular orientations at a coolant inlet temperature of 40 °C, the LHP operated successfully down to a Q_{in} of 15 watts. Successful operation was defined to be a steady evaporator and condenser temperature at a given steady heat input.

ii. Varying Evaporator Angles at 20 °C Coolant Inlet Temperature.

Figure 4.2 contains the varying evaporator angle graphs for the 20 °C coolant inlet temperature where there is no relative height difference between evaporator and condenser. From Figure 4.2, the graphs are fairly tightly grouped for Q_{in} greater than 40 watts. However, below 40 watts the ΔT increases with decreasing Q_{in} , or equivalently, there is a negative slope at the lower Q_{in} values. This negative slope is not found for all angular orientations, but only at those orientations which successfully operated at 15 watts. Only the +135, 0, and -45 degree evaporator angles operated successfully at 15 watts. For the positive slope regions with Q_{in} greater than 40 watts, the ΔT at a given Q_{in}

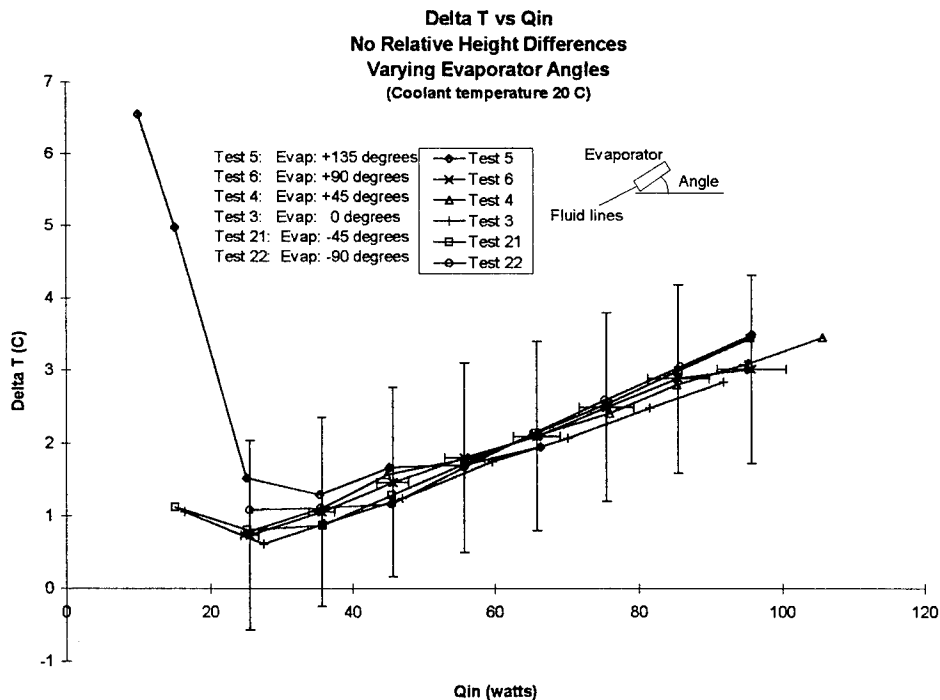


Figure 4.2 Delta T vs Q_{in} , No Relative Height Differences, Varying Evaporator Angles, 20 °C Coolant Temperature

did not vary significantly between the various evaporator angular orientations. The ΔT variation was less than 0.5 °C.

2. Comparison Of Varying Condenser Angles for 20 °C and 40 °C Coolant Inlet Temperatures at No Relative Height Difference. In this section the effects on performance of coolant inlet temperature and condenser angles will be discussed.

i. Varying Condenser Angles at 20 °C Coolant Inlet Temperature. Figure 4.3 contains the varying condenser angle graphs for the 20 °C coolant inlet temperature where there is no relative height difference between evaporator and condenser. In Figure 4.3 one observes a distinct stratification of the graphs, which points to a condenser angular orientation dependence on performance. Here, just as for the varying evaporator angular orientations with a 20 °C coolant inlet temperature (Figure 4.2), below a heat input of 40 watts the slope is generally negative. However, comparing the varying evaporator angular orientations to the varying condenser angular orientations for a 20 °C coolant inlet temperature at a Q_{in} of 15 watts, Figure 4.2 versus Figure 4.3, the LHP successfully operated at all condenser angles, where it did not for all evaporator angles. This may indicate that operation at low Q_{in} is more sensitive to evaporator angular orientations than condenser angular orientations. This is most likely due to the LHPs particular internal construction in combination with the low mass flow rate.

There are two potential explanations for the negative followed by positive slopes of the graphs. The first is given by Dickey and Peterson (1994). They account for the phenomenon using the pressure temperature properties of the working fluid and the Clausius-Clapeyron relationship.

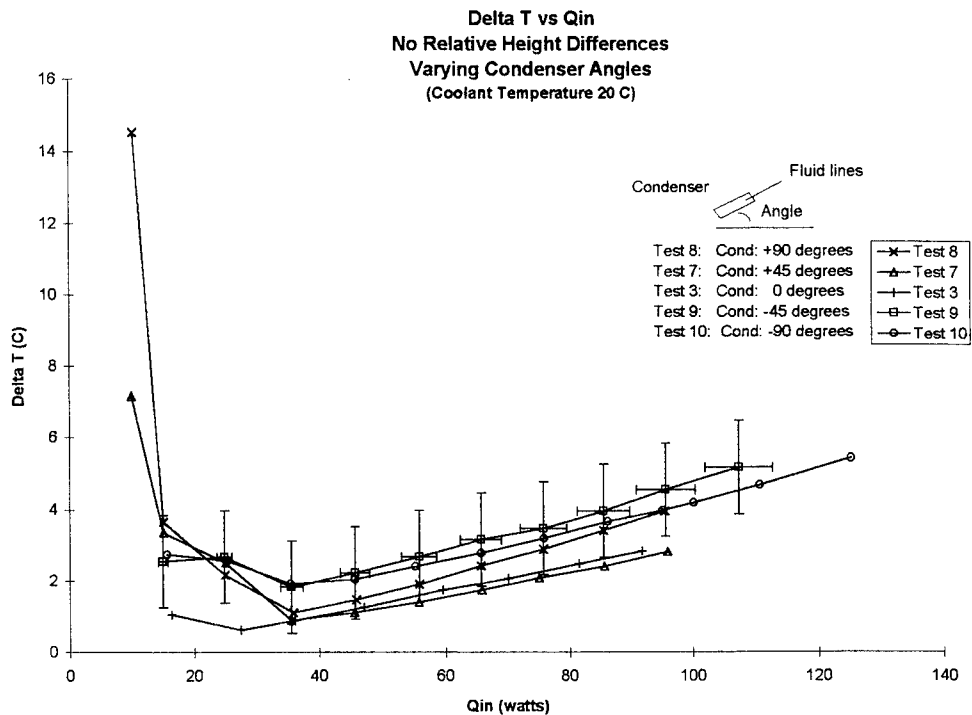


Figure 4.3 Delta T vs Q_{in}, No Relative Height Differences, Varying Condenser Angles, 20 °C Coolant Temperature

The Clausius-Claperon relationship is given as,

$$\Delta P_t = \frac{h_{fg} P_v \Delta T_w}{RT_v^2} \quad \text{Eqn 4.1}$$

where ΔT_w is the temperature difference across the wick, ΔP_t is the pressure difference developed across the wick due to the temperature difference across the wick, P_v is the vapor pressure, T_v is the vapor temperature and R the gas constant for the vapor. For low input power the system pressure must be high enough to account for the small ΔT_w , which is due to the low mass flow rate through the wick. With the low mass flow rate, insufficient sub-cooled liquid reaches the evaporator to maintain much of a temperature difference across the wick. From the Clausius-Claperon relationship, to make up for pressure losses in the LHP, a higher vapor pressure is required. Due to the pressure

temperature properties of the working fluid, the higher vapor pressure can only be attained with a higher temperature, thus a higher evaporator temperature. As the input power is increased there is a larger mass flow rate, with the increased mass flow rate there is an increase in the temperature difference across the wick (due to the sub-cooled liquid on the liquid side of the wick) with a corresponding decrease in the required vapor pressure and a subsequent decrease in vapor temperature.

The second theory explaining the negative slope formation is that the condenser is full of liquid and must be cleared of the liquid to make available surface area for the vapor to condense on. With less vapor condensed, the vapor pressure continues to increase until the pressure is sufficient to push the liquid up and out of the condenser. Again, from the pressure temperature properties of the working fluid, the higher pressure can only be attained with a higher temperature, thus, a higher evaporator temperature.

ii. Varying Condenser Angles at 40 °C Coolant Inlet Temperature.

Figure 4.4 contains the varying condenser angle graphs for the 40 °C coolant inlet temperature where there is no height difference between evaporator and condenser. From Figure 4.4, there is again the stratification of the varying condenser angle graphs as found in Figure 4.3. However, for the 40 °C coolant inlet temperature no real negative slope region of the graphs is evident for either varying evaporator or varying condenser angles (Figure 4.1 and Figure 4.4). This shows a clear dependence of performance on the operating temperature, with the improved performance being for the higher coolant inlet temperatures (improved performance being a smaller ΔT). However, there is a trade off.

At the higher coolant inlet temperatures the LHP cannot transport as much heat due to the maximum operating temperature limit placed on the evaporator.

3. Comparison of Varying Evaporator Angles at Evaporator-Over-Condenser Height Differences of: 0 meters, 1.22 meters, and 2.44 meters. In this section the existence of a negative slope region on the ΔT vs Q_{in} graphs will be discussed along with the shifting of the transition point at which the slope changes from negative to positive. Additionally, the minimum Q_{in} observed for evaporator angles is discussed, and finally the optimum evaporator angle for the minimum ΔT is noted.

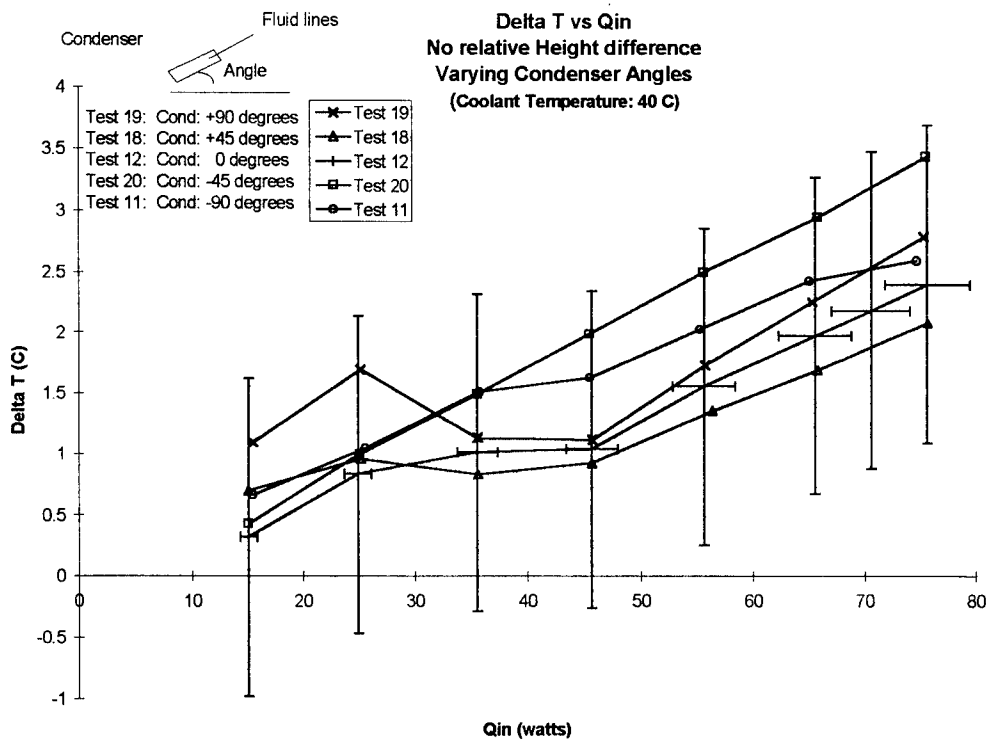


Figure 4.4 Delta T vs Q_{in} , No Relative Height Differences, Varying Condenser Angles, 40 °C Coolant Temperature

i. Varying Evaporator Angles at Evaporator-Over-Condenser Height

Difference of 1.22 meters. Figure 4.5 contains varying evaporator angle graphs for an evaporator-over-condenser height difference (ΔH) of 1.22 meters where the coolant inlet temperature is 20 °C. In Figure 4.5, the Q_{in} point at which the slope transitions from negative to positive, appears to depend on evaporator angular orientation. This is evidenced by the initiation of the negative slope for the 0 degree evaporator angle taking place at a Q_{in} of 45 watts versus the initiation of the negative slopes for the other evaporator angles taking place near 20 watts Q_{in} . Additionally, whether or not there is a transition from a negative to a positive slope appears to be dependent upon evaporator angle. This is shown by the fact that for evaporator angles of +90 and +45 degrees there is no negative slope region. For those evaporator angles with no negative slope, there is an associated increase in the minimum Q_{in} required to maintain LHP operation. For the +90 degree evaporator angle, the LHP would not continue to operate below a Q_{in} of 20 watts and for the +45 orientation the LHP was not operated below a Q_{in} of 45 watts. For the orientations where the LHP has a negative slope, that is at heat inputs of less than 20 watts, the best performance (lowest ΔT) was for the -90 degree evaporator orientation, followed by the -45, and 0 degree orientation. Throughout the positive slope region, above the transition points from negative to positive slope, there is no indication of a performance dependence on evaporator angular orientation.

ii. Varying Evaporator Angles at Evaporator-Over-Condenser Height

Difference of 2.44 meters. Figure 4.6 contains varying evaporator angle graphs for an evaporator-over-condenser height difference of 2.44 meters where the coolant inlet

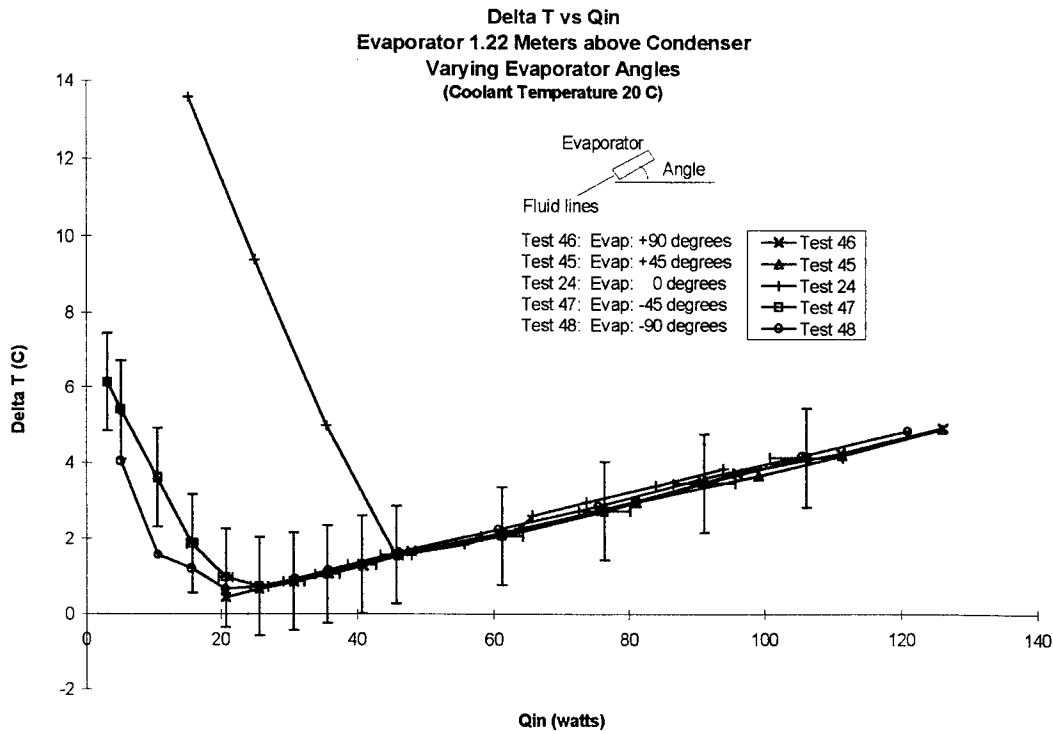


Figure 4.5 Delta T vs Q_{in} , 1.22 meter Height Difference, Varying Evaporator Angles, 20 °C Coolant Temperature

temperature is 20 °C. From Figure 4.6, there are also evaporator angles at which no negative slope is observed. These angles are the same as for the ΔH of 1.22 meters, +95, and +45 degrees (Figure 4.5). For the varying evaporator angles at which there is a negative slope, the transition points are within 10 watts of each other. This indicates that the Q_{in} point at which the slopes change is only slightly dependent upon evaporator angular orientation. In comparison, for a ΔH of 1.22 meters (Figure 4.5), the point at which the slopes shift from negative to positive is much more varied, ranging from 20 watts for two of the evaporator angles to 45 watts for the horizontal evaporator angle.

In general there appeared to be a minimum Q_{in} for each of the evaporator angles where a negative slope failed to develop. Trying to determine what the minimum Q_{in} was

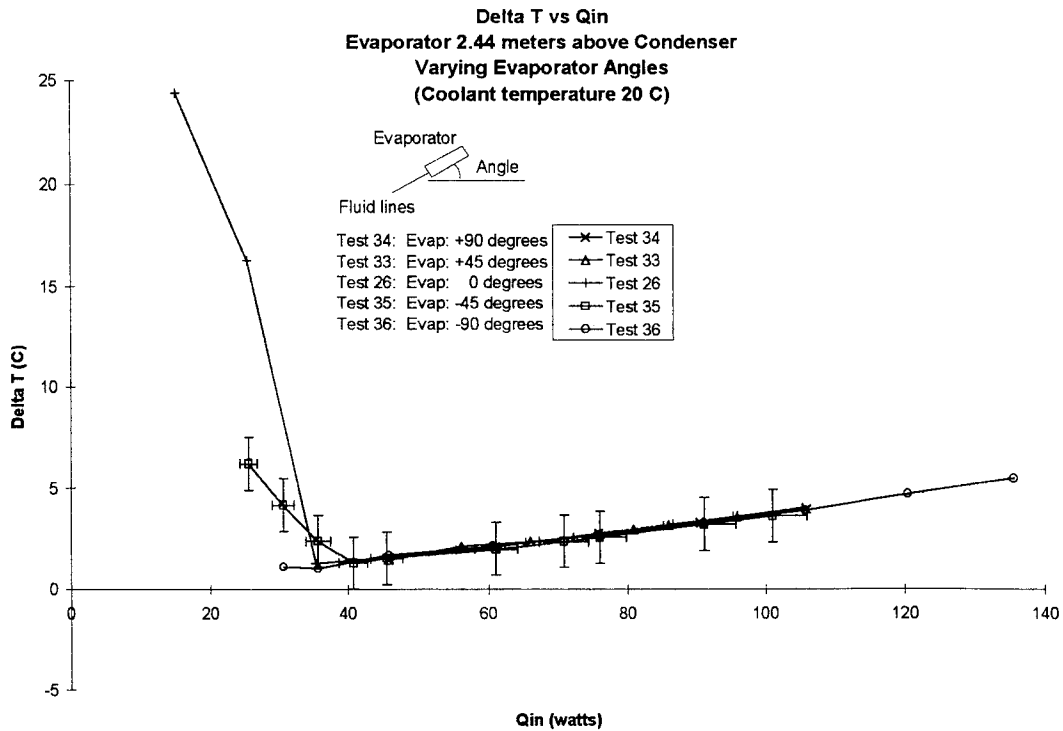


Figure 4.6 ΔT vs Q_{in} , 2.44 meter Height Difference, Varying Evaporator Angles, 20 °C Coolant Temperature

for different ΔH was complicated by the fact that the Q_{in} minimum was found to be sensitive to the rate at which the Q_{in} was reduced. This rate sensitivity was not observed until later on in the testing (this observation is more fully discussed in section 4 B). Thus, a comparison of minimum Q_{in} for the no negative slope evaporator angles between different heights would be of questionable accuracy, but may provide insight to general trends.

Comparing between a ΔH of 1.22 meters and 2.44 meters, for the angles with no negative slope, it was found a greater Q_{in} minimum is required at the greater ΔH , 45 watts versus 20 watts. These Q_{in} minimum are the minimums that were tested at. As mentioned

above, it may be possible to operate the pipe for these orientations at a lower Q_{in} . A summary of the evaporator angles tested and the observance of a negative or positive slope, along with the minimum Q_{in} tested is presented in Table 4.1.

For the orientations where the LHP had a negative slope region at the 2.44 meter ΔH , the best performance (lowest ΔT) was for the -45 degree orientation, followed by the horizontal orientation. The most significant result that these graphs reveal is that for the positive slope region, the performance appears to be independent of evaporator angular orientation, while the formation of a negative slope region does appear to be sensitive to evaporator angular orientations.

A potential explanation for the lack of heat pipe operation at the lower Q_{in} values, for the positive evaporator angles, may be attributed to the placement of the vapor line entrance within the evaporator. The interior design at this point is unknown so one can only speculate. However, what may be occurring is liquid flooding thru the wick, obstructing the entrance to the vapor line. Figure 4.7 shows potential orientations where the vapor line would be obstructed. If liquid is obstructing the vapor line this would require a high vapor pressure, with the associated increased temperature, to push the liquid out of the way or push the liquid down the vapor line. To attain the higher temperatures requires a higher heat input, thus operation is not observed when the Q_{in} is too low to attain the required temperatures.

4. Comparison of Varying Condenser Angles at Evaporator-Over-Condenser Height Differences of: 0 meters, 1.22 meters, and 2.44 meters. This section discusses the minimum Q_{in} operation point found for all condenser angular orientations and height

Evaporator

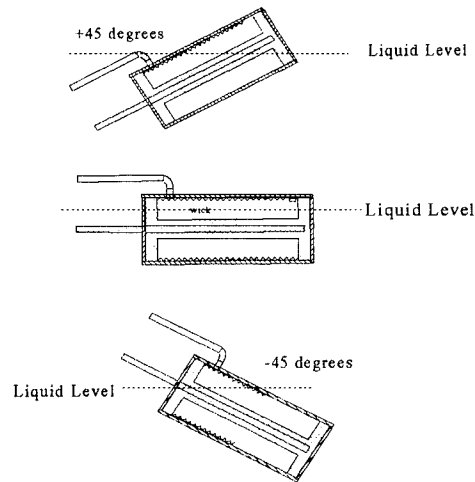


Figure 4.7 Obstruction of Vapor Line

differences, and discusses the existence of negative slope regions and the locations of the transition points where the slopes change from negative to positive.

i. Varying Condenser Angles at Evaporator-Over-Condenser Height Difference of 1.22 meters. Figure 4.8 contains varying condenser angle graphs for an evaporator-over-condenser height difference of 1.22 meters where the coolant inlet temperature is 20 °C. It is observed from Figure 4.8 that the LHP easily reached and maintained steady state operation at a Q_{in} of 15 watts. Additionally, all condenser angular orientations show the negative slope followed by a positive slope for increasing Q_{in} . For all condenser angles, the point at which the slopes change from negative to positive takes place near 45 watts Q_{in} . This is in contrast to the varying evaporator angles at a ΔH of 1.22 meters (Figure 4.5), where the transition point was found to depend upon evaporator angle.

It is interesting to note that the transition point from negative to positive for the

Table 4.1 Varying Evaporator Angles and Heights, Summary Data

Evaporator Angle (degrees)	ΔH (evaporator over condenser) (meters)	Coolant Inlet Temperature ($^{\circ}\text{C}$)	Minimum Q_{in} operated at (watt)	Q_{in} at transition (negative to positive slope)
135	0	40	15	no negative slope
135	0	20	10	35
90	0	40	15	no negative slope
90	0	20	25	no negative slope
90	1.22	20	20	no negative slope
90	2.44	20	45	no negative slope
45	0	40	15	no negative slope
45	0	20	25	no negative slope
45	2.44	20	45	no negative slope
45	1.22	20	45	no negative slope
0	0	40	15	no negative slope
0	0	20	15	25
0	1.22	20	15	45
0	2.44	20	15	35
-45	0	40	15	no negative slope
-45	0	20	15	25
-45	1.22	20	3	25
-45	2.44	20	25	40
-90	0	40	15	no negative slope
-90	0	20	25	no negative slope
-90	1.22	20	5	20
-90	2.44	20	30	35

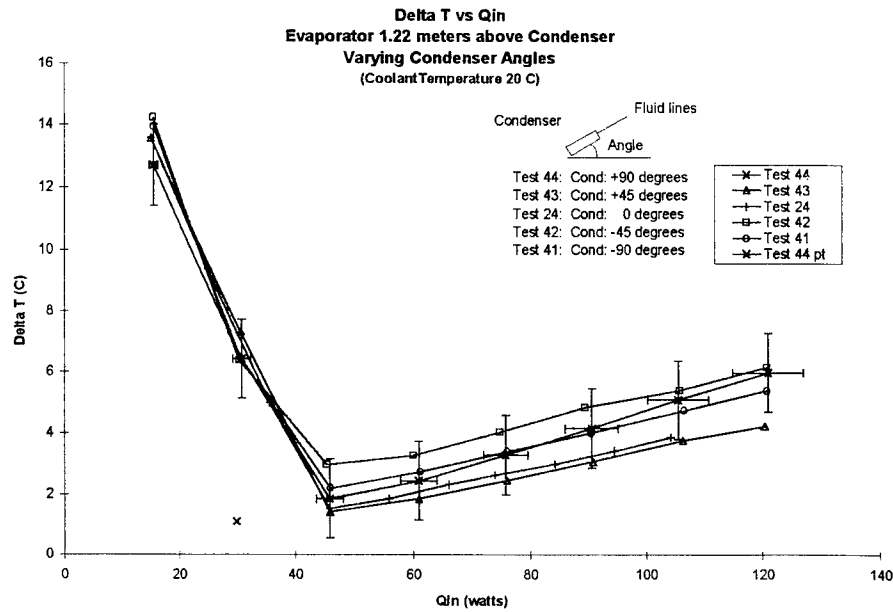


Figure 4.8 Delta T vs Q_{in} , 1.22 meter Height Difference, Varying Condenser Angles, 20 °C Coolant Temperature

condenser at 0 degrees (where both condenser and evaporator are horizontal, test 24) lines up with all the other condenser angle graphs of Figure 4.8. However, when comparing this transition point to the varying evaporator angular orientations at ΔH of 1.22 meters (Figure 4.5), it is at a much higher Q_{in} than for the other evaporator angles (which have a negative to positive slope transition point). This suggests again the influence of evaporator orientation on performance.

ii. Varying Condenser Angles at Evaporator-Over-Condenser Height Difference of 2.44 meters. Figure 4.9 contains varying condenser angle graphs for an evaporator-over-condenser height difference of 2.44 meters where the coolant inlet temperature is 20 °C. It was observed in Figure 4.9, as well as for the ΔH of 1.22 meters,

Figure 4.8, that the LHP reached and maintained steady state operation at a Q_{in} of 15 watts for all condenser angular orientations.

Comparing the varying condenser angle graphs of Figures 4.8 and 4.9, with the exception of the tests for the +45 and 0 degree angles, the two figures show the same general trends. However, the graphs at a ΔH of 2.44 meters show a higher ΔT at the 15 watt Q_{in} than those at a ΔH of 1.22 meters. For the ΔH of 2.44 meters, the ΔT ranges from 18.69 °C to 24.94 °C, and at a ΔH of 1.22 meters the ΔT ranges from 12.71 °C to 15.42 °C. In contrast, when comparing the ΔT at a Q_{in} of 75 watts, there is not as much difference between the two heights; at the ΔH of 2.44 meters the ΔT ranges from 2.34 °C to 3.75 °C, and at a ΔH of 1.22 meters the ΔT ranges from 2.62 °C to 4.02 °C. These

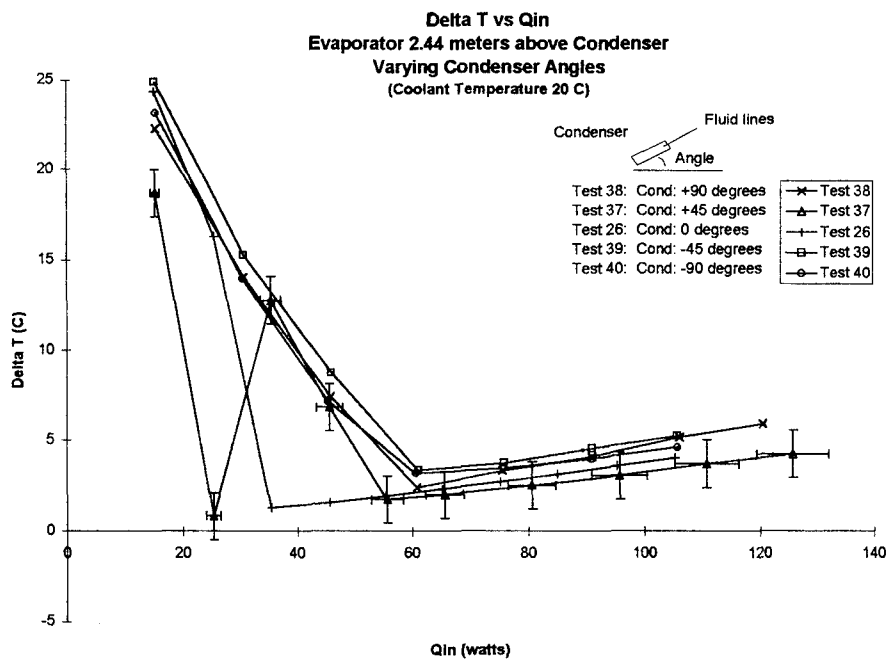


Figure 4.9 Delta T vs Q_{in} , 2.44 meter Height Difference, Varying Condenser Angles, 20 °C Coolant Temperature

results suggest that the height difference has its greatest influence at the low Q_{in} values, or equivalently, in the negative slope region of the graphs.

Of particular interest are the tests for the +45 and 0 degree condenser angles in Figure 4.9. These tests show a departure from what otherwise appears to be the normal trends for the LHP, especially when compared to the graphs of Figure 4.8, where all five graphs follow the same general trend. The departure of the results at 0 and +45 degrees from the other angular orientations indicates either an error in the data or some other phenomenon. Since the experimental procedures were not changed between tests, it is reasonable to eliminate the cause as an error, thus these differences must indicate some other phenomenon. This phenomenon is discussed further in section IV. B as a ΔT anomaly.

iii. Performance Dependence on Condenser Angular Orientation. The performance of the LHP appears to be dependent upon the condenser angular orientation. At certain Q_{in} values, for all ΔH and coolant temperatures the order of the lowest to highest ΔT remains the same, that is to say, the same condenser angle has the highest ΔT , or lowest ΔT .

It is also noted that for all condenser graphs when Q_{in} is above 35 watts, there is a general trend of the +90 angle graphs to cross the -90 graphs. This trend showing the difference in slopes for these two condenser angles further indicates the dependence of performance on the orientation of the condenser. Specifically, it shows that the best orientation for performance, where the condenser is straight up or straight down, changes

with input power. For all condenser angles tested above 35 watts, the best condenser angle for performance (lowest ΔT) is +45 degrees and the poorest is -45 degrees.

Due to the uncertainty in the measurements it could be argued that performance based on condenser angular orientation is insignificant. However, the consistency of the ΔT ordering of the graphs throughout all the relative height and temperature differences, plainly points out such a dependence.

5. Comparison of Varying Relative Heights at Fixed Horizontal Angular

Orientations. The following section discusses the effects of height on LHP performance.

i. Evaporator-Over-Condenser Orientations. Figure 4.10 contains the graphs for varying evaporator-over-condenser height differences where the evaporator and condenser are fixed to the horizontal orientation and the coolant inlet temperature is 20 °C. It is observed in Figure 4.10 that there is a shift in the transition point at which the slope changes from negative to positive. The transition point appears to be related to the ΔH . In general, the transition point shifts right with increasing ΔH , the exception being the plot for the ΔH of 2.44 meters. At this ΔH , the transition point is near 35 watts. However, if this plot is compared to the majority of the graphs for the varying condenser angular orientations at this same ΔH (Figure 4.9) the transition point would be found near 60 watts. This would appropriately place the transition point for the 2.44 meter plot in between the graphs for 1.83 and 2.79 meters, as seen in Figure 4.10 (where the transition point would be shifting right with increasing ΔH or equivalently at a higher Q_{in}). The

misplacement of the 2.44 meter ΔH graph is most likely attributed to the previously mentioned ΔT anomaly.

An additional result found for the various heights, is that once the pipe is operating in the positive slope region, the performance is only slightly related to ΔH . However, there is an order from best to poorest performance, with the best (lowest ΔT) found for no height difference, and the poorest found at the 2.93 meter height difference. In the negative slope region, the best performance is found at the smaller ΔH .

ii. Condenser-Over-Evaporator Orientations. Figure 4.11 contains the graphs for varying condenser-over-evaporator height differences where the evaporator and

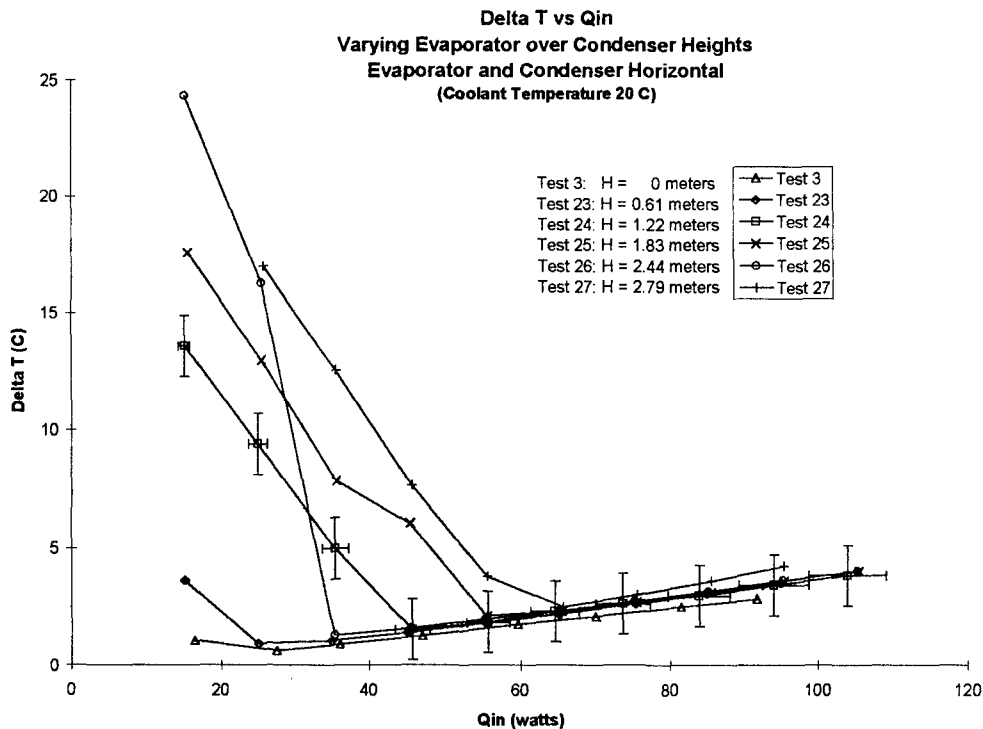


Figure 4.10 Delta T vs Q_{in}, Varying Evaporator over Condenser Heights, Evaporator and Condenser Horizontal, Coolant Temperature 20 °C

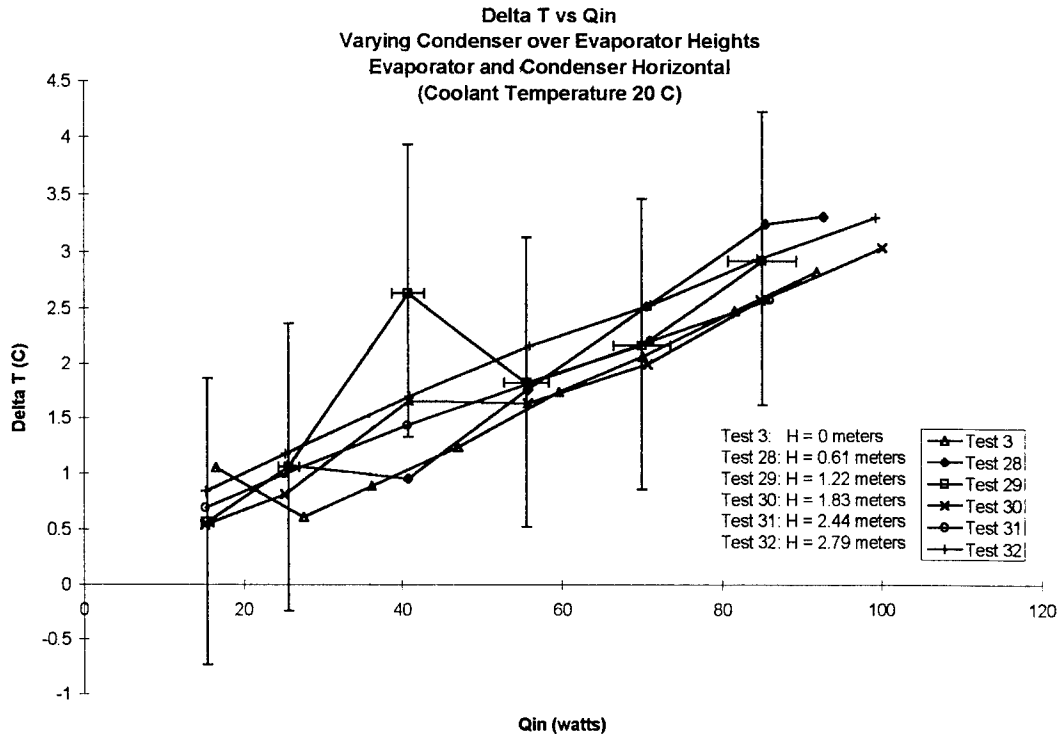


Figure 4.11 Delta T vs Q_{in} , Varying Condenser over Evaporator Heights, Evaporator and Condenser Horizontal, Coolant Temperature 20 °C

condenser are fixed to the horizontal orientation and the coolant inlet temperature is 20 °C. It is observed in Figure 4.11 that the ΔT stayed below 4.0 °C for all heights and Q_{in} tested. Additionally, the LHP continued to operated successfully at 15 watts for all ΔH with the condenser over the evaporator. The data for these tests seems somewhat more sporadic than for other tests. However, the LHP does appear to operate, within the uncertainty bounds, in a positive slope range for all power and height orientations. A potential explanation for the sporadic graphs may be due to the particular orientation of the liquid and vapor lines.

6. Trends Attributable to Coolant Inlet Temperature. This section discusses the effects on performance of coolant inlet temperature. The effects referenced are for the no relative height difference orientations.

i. Summary of Comparison for Varying Evaporator Angles Between 20 °C and 40 °C Coolant Inlet Temperatures at No Relative Height Difference. An interesting difference between the two coolant temperatures for varying evaporator angles (Figures 4.1 and 4.2), is the initiation of a negative slope for some angular orientations at the 20 °C coolant inlet temperature. This negative slope region at the lower Q_{in} values appears to indicate a performance dependence upon operating temperature, since this phenomenon is observed only at the 20 °C coolant inlet temperature. Additionally, the formation of a negative slope region at the lower coolant inlet temperature appears to be related to the evaporator angular orientation. Thus, the evaporator angular influence becomes a factor only when the coolant is below some critical temperature. From Figure 4.2, the negative slope is clearly present at an evaporator angle of +135 degrees. If the uncertainty is neglected, the negative slope is present at 0 and -45 degrees as well.

Another difference observed between the two coolant temperatures for varying evaporator angles is that for the 40 °C coolant inlet temperature the LHP easily operates at the 15 watt Q_{in} for all angular orientations. While at the 20 °C temperature, only half of the angular orientations operated at this low of a Q_{in} . The evaporator angles at which the LHP successfully operated at 15 watts were: +135, 0, and -45 degrees, the same angles at which the negative slope is observed.

ii. Summary for all Angular Orientations. In comparing the ΔT results between 40 °C and 20 °C for all the varying condenser and evaporator angular orientations, above 40 watts there doesn't appear to be a temperature influence on the ΔT . However, below 40 watts at the 20 °C coolant inlet temperature, a negative slope region readily forms for both condenser and evaporator angular orientations.

B. Other Observations

1. Q_{in} Sensitivity. The Q_{in} for each test was initially set high enough to insure LHP start up. Once started, the Q_{in} could then be reduced and the pipe would continue to operate. However, for a given ΔH there appears to be a minimum Q_{in} required for LHP operation.

For many of the tests, keeping the LHP running at the lower Q_{in} values was often a rather delicate operation. LHP operation at the lower Q_{in} is sensitive to the rate at which the Q_{in} is decreased. The greater the Q_{in} step decrease, the greater the possibility that the LHP would become unstable and cease to operate. Unstable was defined as an evaporator temperature increase of 1 °C ~ 3 °C per minute for more than a few minutes. When the pipe was operating in the positive slope region it would easily handle up to a 15 watt step decrease between steady states. However, once the pipe was operating in the negative slope region, step decreases of 5 watts or less were used to insure continued operation.

2. Observation of a ΔT Anomaly. There appears to be a point at which the slope either shifts from positive to negative or remains positive. This is referred to as a ΔT anomaly.

This tendency for the pipe to continue to operate along the positive slope is clearly demonstrated in Figure 4.9 for tests 26 (0 degree condenser angle), and test 37, (+45 degree condenser angle). For test 26 where the condenser angle is horizontal, ΔT continues to decrease with decreasing Q_{in} along the positive slope line. Additionally, for test 37 where the angle is +45 degrees, the 25 watt Q_{in} data point lies on a projection of its positive slope line.

Another test that demonstrates the ΔT anomaly is test 44 (in which the condenser angle is set at +90 at a ΔH of 1.22 meters, Figure 4.8). The pipe was started in the morning and allowed to stabilize for 90 minutes at 30 watts; it stabilized at a ΔT of 1.09 °C. The data acquisition equipment locked up and so the test was reaccomplished for the 30 watt data point later that day. Again the LHP was allowed to stabilize for 90 minutes, however, this time the ΔT was 6.42 °C. Plotting the first point of ΔT of 1.09 °C at 30 watts places it on an extrapolated line drawn from the positive slope region for the +90 degree condenser plot of Figure 4.8.

3. Evaporator Angle Performance Enhancement. For the evaporator angular orientations which developed a negative slope, the ΔT was significantly lower than for condenser angular orientations at the same ΔH and Q_{in} . This is observed for a ΔH of 1.22 meters, where evaporator angular orientations of -45, and -90 degrees operated at a Q_{in} of 15 watts at a ΔT between 4.10 °C and 5.77 °C, where for the same ΔH and Q_{in} the varying condenser angular orientations maintained a ΔT between 12.71 °C and 15.42 °C (Figure 4.5 vs 4.8).

Thus it appears that there exist optimum evaporator angular orientations, in the negative slope region, which improve the performance of the loop heat pipe.

C. Performance Degradation

1. Observed Failure Modes.

i. Sensitivity to Decreases in Input Power. As mentioned above, the LHP is sensitive to the rate of decrease of input power. Further, it appears that depending on the slope at which the LHP is operating (positive or negative) it is more or less sensitive to the step size decrease of power. The LHP is most sensitive to the rate of decrease when operating on the negative slope.

ii. Minimum Q_{in} dependence on Evaporator Angles. The LHP operated successfully at a Q_{in} as low as 15 watts for all condenser angular orientations at both 20 °C and 40 °C coolant inlet temperature. This was not the case for evaporator angular orientations. The LHP operated successfully at all evaporator angular orientations when the coolant inlet temperature was at 40 °C. However, when the coolant inlet temperature was 20 °C, the LHP did not operate consistently at a Q_{in} of 15 watts for all evaporator angles.

2. Performance Degradation with ΔH . The LHP was found to operate at all condenser angular orientations for all heights at a Q_{in} minimum of 15 watts. However, depending on the height, the ΔT at the Q_{in} minimum varied. The ΔT at Q_{in} minimum of 15 watts was found to increase (decreasing performance) with increasing ΔH .

V. Conclusions and Recommendations

The focus of this research has been to determine the effects of varying angular orientation and height on the performance of a loop heat pipe (LHP). The tests performed have enabled the evaluation of LHP performance with respect to: varying evaporator angular orientation, varying condenser angular orientation, different coolant temperatures, and varying relative height difference (ΔH) for evaporator-over-condenser. The following is a summary of the conclusions drawn from this research, followed by recommendations for future work.

A. Conclusions

1. Performance Dependence on Evaporator Angle. The LHP performance was found to be sensitive to the evaporator angle in two areas, the first being whether or not a negative slope region would form, and the second being the heat input (Q_{in}) point at which this negative slope forms. The evaporator angle was found not to influence LHP performance once the Q_{in} was above the transition point (from negative to positive slope region).

2. Performance Dependence on Condenser Angle. The condenser angular orientations appear to have the most consistent effects on performance. Throughout all tests where the Q_{in} was above the transition point (the LHP operating in the positive slope region), the +45 degree angle was found to have the lowest ΔT (best performance) and the -45 degree angle the highest ΔT (poorest performance).

3. Performance Dependence on Coolant Temperature. The most significant influence that coolant temperature had on LHP performance was related to whether or not a negative slope region would form. It was found that for all condenser and evaporator angles, where there was no relative height difference, that at the 40 °C coolant inlet temperature no negative slope region would form, and thus the LHP would operate at the lowest ΔT for the lower Q_{in} values. For all test at a 20 °C coolant inlet temperature a negative slope region formed.

4. Performance Dependence on Relative Heights of Evaporator Over Condenser. It was found that once the pipe was operating in the positive slope region that ΔH had a negligible influence on performance. However, the transition point from negative to positive slope, was found to increase as ΔH increased. This reveals that for an application with a sufficiently high Q_{in} , the relative height will not adversely influence the ability of the pipe to transport heat in a downward direction.

5. Q_{in} Influences. It was found that for some evaporator angular orientations, the LHP would not operate below some minimum Q_{in} . One of the more significant items of interest is the LHP's sensitivity to the rate at which Q_{in} is decreased. When the Q_{in} was decreased too rapidly, the LHP failed to operate. This sensitivity was found to be greater when the LHP was operating in the negative slope region.

This sensitivity to the rate of decrease in Q_{in} , and the minimum Q_{in} required for certain evaporator orientations make this LHP of limited use on aircraft where varying heat fluxes may be experienced.

B. Recommendations:

1. Continue Evaluation of the Sensitivity to Step Decreases in Q_{in} . The pipe was found to be sensitive to the rate at which the heat input was decreased. In order to insure LHPs are suitable for aircraft applications, this sensitivity should be evaluated thoroughly enough to gain an understanding of what factors influence it.

2. Evaluate Performance Dependence on Various Line Routings. All of the testing done and the analysis above has assumed the influence of the line routing to be negligible. A recommendation for future work is to test for various line routing to isolate this influence. This could be accomplished by a series of no-relative-height-difference tests where the condenser and evaporator are drawn together on the mounting bar, causing the 'S' shape of the lines to extend vertically up and down (see Figure 2.1).

3. Continue Evaluation of the ΔT Anomaly. For some of the test where the ΔT anomaly was observed, it was noted the tests were the first of the day, and Q_{in} was at or below the negative to positive slope transition Q_{in} . In this situation the LHP started with a constant temperature throughout. This constant temperature throughout, may have an influence on the ability to operate the LHP in the positive slope region.

A recommendation for future work is to accomplish more tests starting with the LHP at a constant temperature throughout, and starting at a Q_{in} near the transition Q_{in} . The intent of these tests would be to determine the parameters which control the transition from the negative to positive slope. The goal would be to determine a means of

controlling the LHP to operate in the positive slope region at the low values of Q_{in} , where the performance would be improved (lower ΔT) for the lower Q_{in} .

Appendix A: Loop Heat Pipe (LHP) Operation

A. The Loop heat LHP (Gernert & Weidner)

In Figure A.1 the numbers on the Figure represent specific fluid states. Figure A.2 presents a pressure temperature diagram showing the fluid states of Figure A.1.

Point 1 represents the vapor pressure and temperature at the interface of vapor and liquid at the surface of the wick. The vapor is collected in a series of grooves and headers which feed into the vapor line at point 2. As the vapor flows through the passages it continues to heat up, increasing its temperature, thus becoming slightly superheated. The vapor then travels through the vapor line to the condenser, where it enters at point 3. The vapor then condenses and through gravity and/or capillary forces (capillary action due to the taper of the condenser) the liquid migrates to the end of the condenser at point 4. The condensate then enters the liquid return line at point 5.

The vapor pressure then forces the liquid back up through the liquid line into a reservoir section in the evaporator. The evaporator has reservoirs on both ends of the wick connected together through an annular section. This configuration enables liquid to completely surround the wick structure. Ideally the device is made self priming by controlling the volumes of the reservoirs, condenser, and the liquid and vapor lines.

The evaporator is built with the reservoirs on the ends, away from the heat source to ensure the liquid fed to the interior section of the wick remains subcooled. This geometry ensures that upon initial heating the vapor will form in the vapor passageway

and not in the liquid reservoirs. As the vapor forms it displaces the liquid out of the vapor

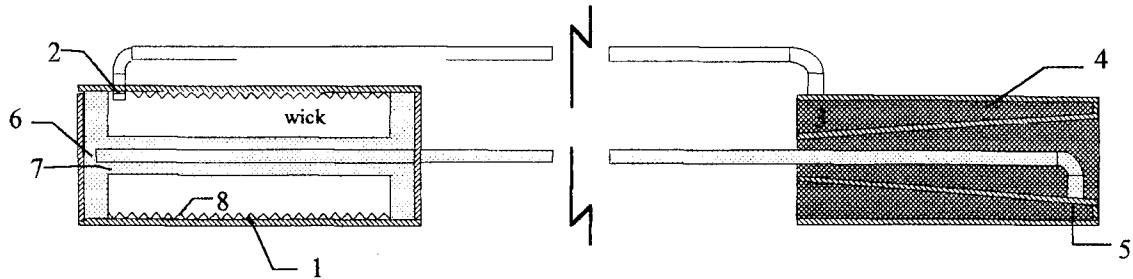


Figure A.1 Loop Heat Pipe

passageways and into the condenser where it is fed through the condenser liquid return line to the reservoirs in the evaporator. Ideally, the volumes and geometry are constructed such that should all the liquid be emptied out of the reservoirs then the liquid would saturate the wick through the vapor lines, thus insuring a self priming device.

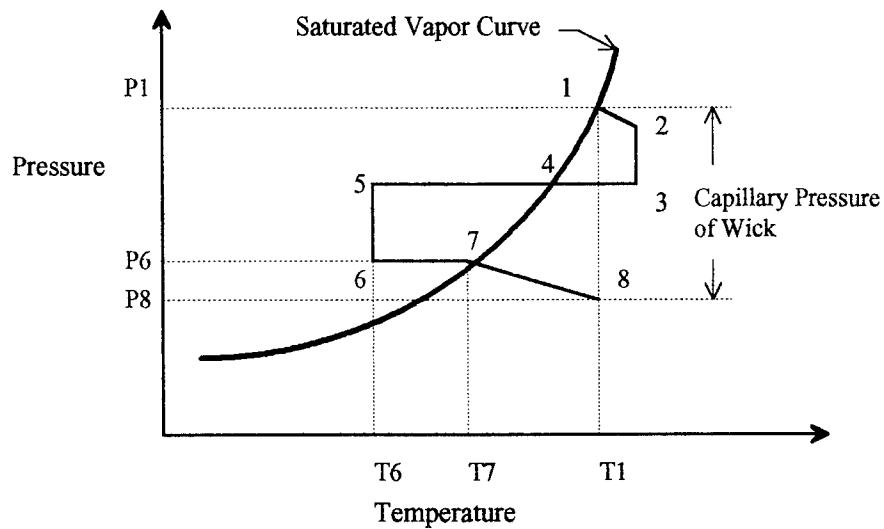


Figure A.2 Operating Cycle of a Loop Heat Pipe

Referencing Figure A.2, point 1 represents the vapor conditions on the wick just above the meniscus surface. The section from one to two (1-2) represents super heating of the vapor as it continues to flow through the vapor passages to the vapor header. The superheating is accompanied by a slight drop in pressure due to viscous forces acting on the vapor as it navigates the vapor passageways. The section from 2-3 represents an adiabatic transport of the vapor through the vapor line to the condenser, again the pressure drop is due to viscous forces acting on the vapor flow. The section from three to four (3-4) represents the vapor entering the condenser and condensing at the saturation pressure, as it condenses the liquid continues to subcool through to point five (5).

The segment from 5-6 represents the liquid returning to the evaporator through the liquid line. The process is represented as being isothermal. The majority of the pressure loss can be attributed to overcoming gravitational head. Section 6-7 represent heating of the liquid in the reservoirs and the wick annulus. Section 7-8 represents the temperature increase and pressure loss as the liquid flows through the wick structure. Point 8 represents the liquid at the surface of the meniscus (vs. point 1 which represents the vapor at the surface of the meniscus). Section 8-1 represents the capillary pressure increase.

In order for the loop heat LHP to operate the capillary pressure, P_c , must be greater than the pressure difference between 8 and 1.

$$\Delta P_c = \frac{2\sigma}{r_c} \geq P_1 - P_8 \quad \text{Eqn 1}$$

Where σ is the fluid's surface tension, and r_c is the effective pore radius of the wick structure.

Appendix B: Sample of Data Recorded

The following pages show a typical spreadsheet which contains the data recorded. This is for Test 44, which had two different steady state operating points as mentioned in Chapter IV.

A
1
2
3
4
5
6
7
8
9
10
11
12
13
14
15
16
17
18
19
20
21
22
23
24
25
26
27
28
29
30
31
32
33
34
35
36
37
38
39
40
41
42
43
44
45
46
47
48
49
50
51
52
53
54
55
56
57
58
59
60
61
62
63
64
65
66
67
68
69
70
71
72
73
74
75
76

	A	B	C	D	E	F	G	H	I	J	K
Test 44			0	1	2	3	5	6	35	36	37
Test 44 Evap: Horizontal	Cond: +90 degrees, bath temp: 20 C										
Evap over Cond by 48 in	Ambient	Evap End	Evap Start	Evap Block	Evap Block	Evap Adia	TC 22/Cond	TC 23/Cond	TC 24/Cond		
09-Aug-94	12:30:47	23.2	35.5	35.9	36.3	36.6	36.1	36.2	25.6	23.1	
09-Aug-94	12:26:47	23.4	35.5	35.9	36.3	36.6	36	36.1	25.6	23.1	
09-Aug-94	12:28:47	23.1	35.5	35.9	36.3	36.5	36	36.1	25.6	23.2	
09-Aug-94	12:24:47	23.5	35.4	35.8	36.2	36.5	35.9	36	25.8	23.1	
09-Aug-94	12:32:47	23	35.5	36	36.3	36.6	36.1	36.1	25.6	23.1	
09-Aug-94	12:44:47	23.1	34.8	35.2	35.8	36.2	35.3	35.4	33	28	
09-Aug-94	12:56:43	23.1	34.4	34.8	35.4	35.8	35	35.1	33	28.3	
09-Aug-94	13:04:47	23.3	34.3	34.7	35.3	35.7	34.9	34.9	33	28.4	
09-Aug-94	13:48:47	23.6	34.2	34.6	35.2	35.6	34.8	34.9	33	28.6	
09-Aug-94	14:18:41	23.7	34.4	34.7	35.4	35.7	34.9	35	33.1	28.6	
09-Aug-94	14:26:47	23.5	34.4	34.8	35.4	35.7	34.9	35	33.2	28.7	
09-Aug-94	12:40:47	23.1	35	35.4	36	36.4	35.5	35.7	32.8	27.7	
09-Aug-94	12:52:47	23.2	34.5	34.9	35.5	35.9	35	35.2	33	28.3	
09-Aug-94	13:14:47	23.3	34.2	34.6	35.2	35.6	34.8	34.9	33	28.5	
09-Aug-94	13:26:47	23.5	34.2	34.6	35.2	35.6	34.8	34.9	33	28.5	
09-Aug-94	13:50:47	24.2	34.2	34.6	35.2	35.6	34.8	34.9	33	28.6	
09-Aug-94	13:10:47	23.1	34.2	34.6	35.2	35.6	34.8	34.9	33	28.5	
09-Aug-94	13:36:41	23.4	34.2	34.6	35.2	35.6	34.8	34.9	33	28.6	
09-Aug-94	12:42:47	23.1	34.9	35.3	35.9	36.3	35.4	35.5	32.9	27.9	
09-Aug-94	12:46:47	23.3	34.7	35.1	35.7	36.1	35.2	35.4	33	28.1	
09-Aug-94	13:00:47	23.4	34.3	34.7	35.4	35.7	34.9	35	33	28.3	
09-Aug-94	13:08:47	23.2	34.2	34.6	35.3	35.6	34.8	34.9	33	28.4	
09-Aug-94	13:38:47	23.4	34.2	34.6	35.3	35.6	34.8	34.9	33	28.6	
09-Aug-94	13:46:47	23.4	34.2	34.6	35.2	35.6	34.8	34.9	33	28.6	
09-Aug-94	13:58:47	23.7	34.3	34.7	35.3	35.7	34.9	35	33.1	28.6	
09-Aug-94	14:28:47	23.8	34.4	34.7	35.4	35.8	34.9	35.1	33.1	28.7	
09-Aug-94	12:54:47	23.6	34.4	34.8	35.5	35.9	35	35.1	33	28.3	
09-Aug-94	13:12:47	23.7	34.2	34.6	35.2	35.6	34.7	34.9	33	28.5	
09-Aug-94	13:30:47	23.4	34.2	34.6	35.2	35.6	34.8	34.9	33	28.6	
09-Aug-94	13:44:47	23.4	34.2	34.6	35.2	35.6	34.8	34.9	33	28.6	
09-Aug-94	13:56:47	23.4	34.3	34.7	35.3	35.7	34.8	35	33	28.5	
09-Aug-94	14:04:47	23.4	34.3	34.7	35.3	35.7	34.9	35	33.1	28.6	
09-Aug-94	14:10:47	24	34.3	34.7	35.3	35.7	34.9	35	33.1	28.6	
09-Aug-94	14:32:47	23.8	34.4	34.8	35.4	35.8	34.9	35	33.2	28.7	
09-Aug-94	14:12:41	23.4	34.3	34.7	35.3	35.7	34.9	35	33.1	28.6	
09-Aug-94	12:48:47	23.1	34.6	35	35.6	36	35.1	35.3	33	28.2	
09-Aug-94	13:02:47	23.2	34.3	34.7	35.3	35.7	34.9	35	33	28.4	
09-Aug-94	13:16:47	24.1	34.2	34.6	35.2	35.6	34.7	34.9	33	28.5	
09-Aug-94	13:18:47	23.4	34.2	34.6	35.2	35.6	34.7	34.9	33	28.5	
09-Aug-94	13:24:47	23.4	34.2	34.6	35.2	35.6	34.8	34.9	33	28.5	
09-Aug-94	13:34:47	23.3	34.2	34.6	35.2	35.6	34.8	34.9	33	28.6	
09-Aug-94	14:20:47	23.5	34.4	34.8	35.4	35.7	34.9	35	33.1	28.7	
09-Aug-94	14:30:47	23.7	34.4	34.8	35.4	35.8	34.9	35	33.2	28.7	
09-Aug-94	13:20:47	23.3	34.2	34.6	35.2	35.6	34.8	34.9	33	28.6	
09-Aug-94	14:02:47	23.6	34.3	34.7	35.3	35.7	34.8	35	33.1	28.6	
09-Aug-94	14:06:47	23.4	34.3	34.7	35.3	35.7	34.9	35	33.1	28.6	
09-Aug-94	14:24:47	23.5	34.4	34.8	35.4	35.8	34.9	35.1	33.2	28.7	
09-Aug-94	12:58:47	23.2	34.4	34.7	35.4	35.8	34.9	35	33	28.3	
09-Aug-94	13:06:47	23.4	34.3	34.7	35.3	35.7	34.8	35	33	28.4	
09-Aug-94	13:40:47	23.3	34.2	34.6	35.2	35.6	34.8	34.9	33.1	28.6	
09-Aug-94	13:42:47	23.6	34.2	34.6	35.2	35.6	34.8	34.9	33	28.6	
09-Aug-94	13:54:47	23.6	34.3	34.7	35.3	35.7	34.8	35	33.1	28.6	
09-Aug-94	14:14:41	23.5	34.3	34.8	35.4	35.7	34.9	35	33.1	28.6	
09-Aug-94	14:22:47	23.6	34.4	34.8	35.4	35.8	34.9	35	33.2	28.7	
09-Aug-94	12:50:41	23.2	34.5	34.9	35.6	35.9	35.1	35.2	33	28.2	
09-Aug-94	13:22:47	23.3	34.2	34.6	35.2	35.6	34.7	34.9	33	28.5	
09-Aug-94	13:28:41	23.5	34.2	34.6	35.2	35.6	34.8	34.9	33	28.5	
09-Aug-94	13:32:47	23.8	34.2	34.6	35.2	35.6	34.8	34.9	33	28.6	
09-Aug-94	14:08:47	23.6	34.3	34.7	35.3	35.7	34.8	35	33.1	28.7	
09-Aug-94	13:52:47	23.8	34.3	34.7	35.3	35.6	34.8	34.9	33	28.6	
09-Aug-94	14:00:47	23.6	34.3	34.7	35.3	35.7	34.9	35	33.1	28.6	
09-Aug-94	14:16:41	23.5	34.3	34.7	35.3	35.7	34.9	35	33.1	28.6	
09-Aug-94	14:34:47	23.5	34.4	34.8	35.4	35.8	34.9	35.1	33.2	28.7	
08-Aug-94	16:21:31	24.2	35	35.3	36.2	36.7	35.5	35.7	34.6	34.7	
08-Aug-94	16:19:31	23.6	35.5	35.7	36.5	37	35.9	36	34.9	34.9	
08-Aug-94	16:39:31	23.5	33.4	34.4	35.3	35.7	34.6	34.8	33.7	33.9	
08-Aug-94	16:23:31	23.5	34.7	35.1	36	36.5	35.3	35.5	34.4	34.5	
08-Aug-94	16:41:31	23.5	33.4	34.4	35.3	35.7	34.8	34.9	33.7	33.9	
08-Aug-94	16:37:25	23.6	33.3	34.4	35.3	35.7	34.6	34.8	33.7	33.9	
08-Aug-94	16:17:31	23.9	35.7	36	36.9	37.4	36.2	36.4	35.2	35.2	
08-Aug-94	16:33:31	23.8	33.4	34.3	35.2	35.6	34.6	34.8	33.7	33.8	
08-Aug-94	16:31:31	24.1	33.6	34.3	35.3	35.7	34.6	34.8	33.7	33.9	

A	L	M	N	O	P	Q	R	S	T	U
1										
2	38	39	40	50	51	60	61	70	71	72
3										Test 44
4	TC 25/Cond	TC 26/Cond	TC 27/Coolin	Coolin Intrp	Coolout Intrp	Specific Heat	Density	Flow rate vol	Heater current	Qin (watts)
5	22.3	22.3	20.205	20.799	21.571	4.1814	0.998	0.703	0.42	15.485
6	22.3	22.2	20.23	20.824	21.623	4.1813	0.998	0.709	0.42	15.521
7	22.4	22.3	20.22	20.814	21.641	4.1813	0.998	0.71	0.42	15.521
8	22.3	22.2	20.153	20.746	21.561	4.1814	0.998	0.718	0.42	15.557
9	22.4	22.3	20.244	20.837	21.61	4.1813	0.998	0.699	0.42	15.557
10	25.4	24.8	20.202	20.796	23.261	4.181	0.9978	0.71	0.59	30.469
11	25.6	25	20.221	20.815	23.513	4.1809	0.9977	0.713	0.59	30.57
12	26.7	25.1	20.244	20.838	23.387	4.1809	0.9977	0.703	0.59	30.57
13	25.8	25.2	20.275	20.869	23.258	4.181	0.9978	0.703	0.59	30.57
14	25.9	25.2	20.316	20.91	23.634	4.1809	0.9977	0.69	0.59	30.57
15	26	25.3	20.337	20.931	23.6	4.1809	0.9977	0.689	0.59	30.57
16	25.3	24.6	20.19	20.784	23.128	4.181	0.9978	0.728	0.59	30.662
17	25.6	24.9	20.221	20.815	23.277	4.181	0.9978	0.699	0.59	30.662
18	25.8	25.1	20.268	20.862	23.368	4.1809	0.9977	0.7	0.59	30.662
19	25.9	25.2	20.287	20.881	23.343	4.1809	0.9977	0.694	0.59	30.662
20	25.8	25.2	20.289	20.883	23.598	4.1809	0.9977	0.703	0.59	30.662
21	25.8	25.1	20.287	20.881	23.557	4.1809	0.9977	0.699	0.59	30.712
22	25.9	25.2	20.268	20.862	23.384	4.1809	0.9977	0.691	0.59	30.712
23	25.3	24.7	20.229	20.823	23.254	4.181	0.9978	0.725	0.59	30.763
24	25.5	24.8	20.214	20.808	23.342	4.1809	0.9978	0.703	0.59	30.763
25	25.7	25	20.217	20.811	23.448	4.1809	0.9977	0.71	0.59	30.763
26	25.7	25.1	20.264	20.857	23.376	4.1809	0.9977	0.699	0.59	30.763
27	25.9	25.2	20.295	20.889	23.6	4.1809	0.9977	0.689	0.59	30.763
28	25.9	25.2	20.278	20.872	23.513	4.1809	0.9977	0.71	0.59	30.763
29	25.9	25.2	20.284	20.878	23.492	4.1809	0.9977	0.7	0.59	30.763
30	26	25.3	20.321	20.915	23.449	4.1809	0.9977	0.689	0.59	30.763
31	25.8	25	20.26	20.854	23.471	4.1809	0.9977	0.713	0.59	30.814
32	25.8	25.1	20.253	20.847	23.309	4.1809	0.9978	0.7	0.59	30.814
33	25.8	25.2	20.287	20.881	23.472	4.1809	0.9977	0.689	0.59	30.814
34	25.9	25.2	20.263	20.857	23.273	4.181	0.9978	0.709	0.59	30.814
35	25.9	25.2	20.281	20.875	23.492	4.1809	0.9977	0.7	0.59	30.814
36	25.9	25.2	20.293	20.887	23.363	4.1809	0.9977	0.699	0.59	30.814
37	25.9	25.2	20.283	20.877	23.58	4.1809	0.9977	0.694	0.59	30.814
38	26	25.3	20.333	20.927	23.671	4.1808	0.9977	0.684	0.59	30.814
39	25.9	25.2	20.326	20.92	23.567	4.1809	0.9977	0.689	0.59	30.855
40	25.5	24.9	20.23	20.824	23.485	4.1809	0.9977	0.704	0.59	30.865
41	25.7	25	20.237	20.831	23.338	4.1809	0.9978	0.71	0.59	30.865
42	25.8	25.1	20.253	20.847	23.439	4.1809	0.9977	0.699	0.59	30.865
43	25.8	25.1	20.245	20.839	23.57	4.1809	0.9977	0.695	0.59	30.865
44	25.8	25.2	20.269	20.863	23.518	4.1809	0.9977	0.694	0.59	30.865
45	25.9	25.2	20.283	20.877	23.468	4.1809	0.9977	0.694	0.59	30.865
46	26	25.3	20.323	20.917	23.378	4.1809	0.9977	0.694	0.59	30.865
47	25.9	25.3	20.322	20.916	23.587	4.1809	0.9977	0.689	0.59	30.865
48	25.8	25.2	20.241	20.835	23.481	4.1809	0.9977	0.694	0.59	30.906
49	25.9	25.2	20.304	20.898	23.509	4.1809	0.9977	0.699	0.59	30.906
50	25.9	25.2	20.295	20.889	23.435	4.1809	0.9977	0.69	0.59	30.906
51	26	25.3	20.323	20.917	23.45	4.1809	0.9977	0.691	0.59	30.906
52	25.7	25	20.234	20.828	23.32	4.1809	0.9978	0.71	0.59	30.957
53	25.7	25.1	20.24	20.834	23.353	4.1809	0.9977	0.699	0.59	30.957
54	25.9	25.2	20.264	20.858	23.365	4.1809	0.9977	0.684	0.59	30.957
55	25.9	25.2	20.298	20.892	23.471	4.1809	0.9977	0.684	0.59	30.957
56	25.9	25.2	20.297	20.891	23.591	4.1809	0.9977	0.699	0.59	30.957
57	25.9	25.2	20.298	20.892	23.592	4.1809	0.9977	0.694	0.59	30.957
58	26	25.3	20.322	20.916	23.587	4.1809	0.9977	0.69	0.59	30.957
59	25.6	24.9	20.22	20.814	23.318	4.1809	0.9978	0.699	0.59	31.008
60	25.9	25.2	20.26	20.854	23.573	4.1809	0.9977	0.694	0.59	31.008
61	25.8	25.2	20.256	20.85	23.415	4.1809	0.9977	0.69	0.59	31.008
62	25.9	25.2	20.249	20.843	23.289	4.1809	0.9978	0.69	0.59	31.008
63	25.9	25.2	20.296	20.89	23.336	4.1809	0.9977	0.694	0.59	31.008
64	25.9	25.2	20.262	20.856	23.611	4.1809	0.9977	0.699	0.59	31.059
65	25.9	25.2	20.301	20.895	23.356	4.1809	0.9977	0.695	0.59	31.059
66	25.9	25.3	20.328	20.922	23.455	4.1809	0.9977	0.693	0.59	31.059
67	26	25.3	20.306	20.9	23.449	4.1809	0.9977	0.685	0.59	31.059
68	34.3	33.6	20.221	20.815	24.822	4.1806	0.9976	0.734	0.72	45.513
69	34.1	32.7	20.195	20.789	24.708	4.1806	0.9976	0.734	0.72	45.686
70	33.7	35	20.243	20.836	24.54	4.1807	0.9976	0.725	0.72	45.686
71	34.3	34.9	20.222	20.816	24.735	4.1806	0.9976	0.735	0.72	45.748
72	33.7	35	20.192	20.786	24.386	4.1807	0.9976	0.729	0.72	45.748
73	33.7	35	20.21	20.804	24.361	4.1807	0.9976	0.725	0.72	45.86
74	33.9	31.9	20.194	20.788	24.534	4.1807	0.9976	0.735	0.72	45.922
75	33.7	34.9	20.205	20.799	24.326	4.1807	0.9976	0.729	0.72	45.922
76	33.7	34.9	20.224	20.818	24.403	4.1807	0.9976	0.729	0.72	46.096

A	X	Y	Z	AA	AB	AC	AD	AE	AF	AG	AH
1											
2			73	74	75	76	77	78	79		
3			Test 44	Test 44	Test 44	Test 44	Test 44	Test 44	Test 44		
4	Qin avg	Qin stdev	PM	Heat Flow out	Heat loss	% loss	Evap Avg	Cond Avg	Delta T	Delta T avg	Delta T stdev
5	0	0	0.141	7.557	7.927	51.19	36.447	23.69	12.76	0	0
6	0	0	0.142	7.889	7.631	49.17	36.418	23.689	12.73	0	0
7	0	0	0.142	8.166	7.355	47.39	36.411	23.72	12.69	0	0
8	0	0	0.144	8.138	7.419	47.69	36.34	23.742	12.6	0	0
9	15.528	0.0301	0.14	7.514	8.043	51.7	36.463	23.694	12.77	12.709	0.0690036
10	0	0	0.142	24.329	6.14	20.15	35.993	28.788	7.205	0	0
11	0	0	0.143	26.745	3.825	12.51	35.611	28.968	6.643	0	0
12	0	0	0.141	24.933	5.637	18.44	35.525	29.024	6.501	0	0
13	0	0	0.141	23.37	7.201	23.55	35.419	29.153	6.266	0	0
14	0	0	0.138	26.135	4.435	14.51	35.555	29.212	6.343	0	0
15	0	0	0.138	25.585	4.985	16.31	35.55	29.279	6.271	0	0
16	0	0	0.146	23.742	6.92	22.57	36.201	28.609	7.592	0	0
17	0	0	0.14	23.939	6.722	21.92	35.691	28.961	6.73	0	0
18	0	0	0.14	24.399	6.263	20.43	35.408	29.089	6.319	0	0
19	0	0	0.139	23.74	6.922	22.58	35.425	29.123	6.302	0	0
20	0	0	0.141	26.555	4.107	13.39	35.434	29.155	6.279	0	0
21	0	0	0.14	26.022	4.69	15.27	35.43	29.085	6.344	0	0
22	0	0	0.138	24.22	6.492	21.14	35.431	29.185	6.246	0	0
23	0	0	0.145	24.508	6.255	20.33	36.081	28.694	7.387	0	0
24	0	0	0.141	24.769	5.994	19.48	35.902	28.858	7.044	0	0
25	0	0	0.142	26.028	4.735	15.39	35.543	28.987	6.556	0	0
26	0	0	0.14	24.495	6.268	20.37	35.451	29.039	6.412	0	0
27	0	0	0.138	25.992	4.771	15.51	35.442	29.162	6.28	0	0
28	0	0	0.142	26.066	4.697	15.27	35.423	29.167	6.256	0	0
29	0	0	0.14	25.442	5.321	17.3	35.501	29.171	6.33	0	0
30	0	0	0.138	24.291	6.472	21.04	35.562	29.274	6.288	0	0
31	0	0	0.143	25.961	4.853	15.75	35.654	28.989	6.665	0	0
32	0	0	0.14	23.959	6.855	22.25	35.405	29.1	6.304	0	0
33	0	0	0.138	24.832	5.982	19.41	35.408	29.152	6.256	0	0
34	0	0	0.142	23.829	6.985	22.67	35.422	29.161	6.26	0	0
35	0	0	0.14	25.472	5.342	17.34	35.486	29.15	6.335	0	0
36	0	0	0.14	24.083	6.731	21.85	35.494	29.207	6.287	0	0
37	0	0	0.139	26.083	4.731	15.35	35.512	29.219	6.293	0	0
38	0	0	0.137	26.117	4.697	15.24	35.572	29.278	6.295	0	0
39	0	0	0.138	25.377	5.478	17.75	35.512	29.215	6.297	0	0
40	0	0	0.141	26.047	4.818	15.61	35.819	28.906	6.914	0	0
41	0	0	0.142	24.745	6.12	19.83	35.518	29.025	6.493	0	0
42	0	0	0.14	25.201	5.664	18.35	35.387	29.089	6.298	0	0
43	0	0	0.139	26.385	4.48	14.51	35.372	29.108	6.264	0	0
44	0	0	0.139	25.627	5.238	16.97	35.409	29.118	6.291	0	0
45	0	0	0.139	25.005	5.86	18.99	35.408	29.179	6.229	0	0
46	0	0	0.139	23.738	7.127	23.09	35.552	29.252	6.23	0	0
47	0	0	0.138	25.606	5.259	17.04	35.569	29.261	6.308	0	0
48	0	0	0.139	25.522	5.384	17.42	35.397	29.122	6.274	0	0
49	0	0	0.14	25.392	5.513	17.84	35.512	29.191	6.321	0	0
50	0	0	0.138	24.43	6.476	20.95	35.499	29.221	6.278	0	0
51	0	0	0.138	24.334	6.572	21.26	35.559	29.291	6.268	0	0
52	0	0	0.142	24.596	6.36	20.55	35.559	28.984	6.576	0	0
53	0	0	0.14	24.496	6.46	20.87	35.49	29.02	6.47	0	0
54	0	0	0.137	23.833	7.124	23.01	35.43	29.18	6.25	0	0
55	0	0	0.137	24.512	6.445	20.82	35.44	29.182	6.258	0	0
56	0	0	0.14	26.261	4.695	15.17	35.479	29.161	6.318	0	0
57	0	0	0.139	26.044	4.913	15.87	35.555	29.221	6.334	0	0
58	0	0	0.138	25.628	5.329	17.21	35.559	29.262	6.297	0	0
59	0	0	0.14	24.351	6.657	21.47	35.747	28.938	6.809	0	0
60	0	0	0.139	26.24	4.767	15.38	35.396	29.127	6.269	0	0
61	0	0	0.138	24.605	6.402	20.65	35.421	29.108	6.314	0	0
62	0	0	0.138	23.475	7.532	24.29	35.413	29.169	6.244	0	0
63	0	0	0.139	23.61	7.397	23.86	35.504	29.223	6.282	0	0
64	0	0	0.14	26.789	4.269	13.75	35.454	29.183	6.272	0	0
65	0	0	0.139	23.777	7.282	23.45	35.535	29.163	6.371	0	0
66	0	0	0.139	24.415	6.644	21.39	35.539	29.231	6.309	0	0
67	30.828	0.1445	0.137	24.294	6.765	21.78	35.587	29.263	6.323	6.42276	0.28794
68	0	0	0.147	40.904	4.609	10.13	36.438	34.539	1.897	0	0
69	0	0	0.147	40.005	5.681	12.43	36.767	34.66	2.107	0	0
70	0	0	0.145	37.326	8.36	18.3	35.489	33.79	1.698	0	0
71	0	0	0.147	40.032	5.716	12.5	36.221	34.426	1.795	0	0
72	0	0	0.146	36.486	9.262	20.25	35.519	33.801	1.719	0	0
73	0	0	0.145	35.866	10.004	21.81	35.501	33.783	1.718	0	0
74	0	0	0.147	38.263	7.659	16.68	37.146	34.765	2.381	0	0
75	0	0	0.146	35.747	10.175	22.16	35.447	33.756	1.691	0	0
76	0	0	0.146	36.332	9.763	21.18	35.459	33.756	1.703	0	0

A	B	C	D	E	F	G	H	I	J	K	
1	Test 44										
2		0	1	2	3	5	6	35	36	37	
3	Test 44	Evap: Horizontal	Cond: +90 degrees	bath temp: 20	C				35		
4	Evap over	Cond by 48 inc	Ambient	Evap End	Evap Start	Evap Block	Evap Block	Evap Adia	TC 22/Cond	TC 23/Cond	TC 24/Cond
77	08-Aug-94	16:35:31	23.3	33.5	34.4	35.3	35.7	34.6	34.8	33.7	33.9
78	08-Aug-94	16:05:31	23.8	38.1	38.7	39.7	40.3	38.9	39.1	37.5	37.7
79	08-Aug-94	16:01:31	23.3	38.4	38.8	39.8	40.4	39	39.2	37.6	37.9
80	08-Aug-94	15:59:25	23.4	38.3	38.9	39.9	40.5	39	39.2	37.7	37.9
81	08-Aug-94	16:03:31	23.3	38.3	38.7	39.8	40.3	38.9	39.1	37.6	37.8
82	08-Aug-94	15:57:31	23.4	38.4	39	40	40.6	39.2	39.3	37.8	38
83	08-Aug-94	15:45:31	23.4	41.9	42.8	44.2	44.9	43	43.2	41.1	41.4
84	08-Aug-94	15:39:31	23.6	42.2	43	44.3	45	43.2	43.3	41.3	41.5
85	08-Aug-94	15:43:31	23.4	41.9	42.8	44.2	44.9	43.1	43.2	41.2	41.4
86	08-Aug-94	15:41:31	23.4	42.1	42.9	44.3	44.9	43.1	43.3	41.2	41.5
87	08-Aug-94	15:37:31	23.5	42.3	43.1	44.4	45.1	43.2	43.4	41.4	41.6
88	08-Aug-94	15:21:31	23.7	45.7	46.9	48.5	49.3	47.1	47.2	44.6	44.9
89	08-Aug-94	15:19:31	23.4	45.8	47	48.6	49.4	47.2	47.3	44.7	45
90	08-Aug-94	15:23:31	23.3	45.6	46.8	48.4	49.2	47	47.2	44.6	44.9
91	08-Aug-94	15:17:31	23.3	46.1	47.1	48.7	49.4	47.2	47.4	44.8	45.1
92	08-Aug-94	15:25:31	23.5	45.6	46.8	48.4	49.2	47	47.1	44.5	44.8
93	08-Aug-94	14:55:31	23.2	49.5	50.9	52.7	53.6	51	51.1	47.9	48.3
94	08-Aug-94	15:01:31	23.1	49.3	50.7	52.6	53.5	50.9	51	47.8	48.2
95	08-Aug-94	15:03:31	23.4	49.3	50.7	52.6	53.5	50.9	51	47.8	48.2
96	08-Aug-94	14:57:25	23.4	49.4	50.8	52.6	53.5	51	51.1	47.8	48.2
97	08-Aug-94	14:59:31	23.7	49.3	50.7	52.6	53.5	50.9	51.1	47.8	48.2
98	08-Aug-94	15:05:31	23.3	49.2	50.7	52.6	53.5	50.9	51	47.8	48.2
99	08-Aug-94	14:33:31	23.1	53.3	55.1	57.2	58.2	55.2	55.3	51.4	51.9
100	08-Aug-94	14:27:31	23.1	53	54.8	56.9	57.9	55	55.1	51.2	51.7
101	08-Aug-94	14:29:31	23.1	53.1	54.9	57	58	55.1	55.2	51.3	51.8
102	08-Aug-94	14:37:31	23.2	53.4	55.1	57.3	58.3	55.3	55.5	51.5	52.1
103	08-Aug-94	14:31:31	23	53.2	55	57.1	58.1	55.2	55.2	51.3	51.9
104	08-Aug-94	14:35:31	23.2	53.3	55.1	57.2	58.2	55.3	55.3	51.5	52
105	08-Aug-94	14:25:31	23.1	52.9	54.7	56.9	57.8	54.9	55	51.2	51.7
106	08-Aug-94	14:39:31	23.5	53.5	55.2	57.4	58.3	55.4	55.5	51.6	52.1
107											
108	08-Aug-94	10:23:00									
109	08-Aug-94	10:25:00									
110	08-Aug-94	10:27:00									
111	08-Aug-94	10:29:00									
112	08-Aug-94	10:31:00									

A
1
2
3
4
77
78
79
80
81
82
83
84
85
86
87
88
89
90
91
92
93
94
95
96
97
98
99
100
101
102
103
104
105
106
107
108
109
110
111
112

	L	M	N	O	P	Q	R	S	T	U
	38	39	40	50	51	60	61	70	71	72
										Test 44
	TC 25/Cond	TC 26/Cond	TC 27/Coolin	Coolin Intrap	Coolout Intrap	Specific Heat	Density	Flow rate vol	Heater current	Qin (watts)
	33.7	34.9	20.217	20.811	24.526	4.1807	0.9976	0.728	0.72	46.096
	37.6	39.2	20.208	20.802	25.432	4.1805	0.9975	0.739	0.83	60.589
	37.6	39.3	20.197	20.791	25.406	4.1805	0.9975	0.739	0.83	60.646
	37.7	39.4	20.212	20.806	25.42	4.1805	0.9975	0.739	0.83	60.861
	37.6	39.2	20.2	20.793	25.68	4.1804	0.9975	0.738	0.83	61.133
	37.8	39.5	20.165	20.759	25.373	4.1805	0.9975	0.738	0.83	61.262
	41.2	43.3	20.176	20.77	26.492	4.1802	0.9974	0.745	0.92	75.365
	41.3	43.5	20.191	20.784	26.566	4.1802	0.9974	0.748	0.93	75.588
	41.3	43.4	20.187	20.781	26.389	4.1803	0.9974	0.745	0.93	75.811
	41.3	43.4	20.186	20.78	26.207	4.1803	0.9974	0.745	0.93	75.971
	41.4	43.6	20.189	20.782	26.364	4.1803	0.9974	0.748	0.93	76.194
	44.7	47.4	20.166	20.759	27.45	4.18	0.9973	0.76	1.01	90.491
	44.9	47.4	20.202	20.796	27.768	4.1799	0.9972	0.754	1.01	90.578
	44.7	47.3	20.187	20.78	27.414	4.18	0.9973	0.754	1.01	90.578
	44.8	47.5	20.167	20.761	27.609	4.18	0.9973	0.76	1.01	90.665
	44.6	47.3	20.192	20.785	27.106	4.1801	0.9973	0.749	1.01	90.752
	48	51.3	20.166	20.76	28.401	4.1798	0.9972	0.764	1.09	105.3
	47.9	51.2	20.145	20.738	28.125	4.1799	0.9972	0.764	1.09	105.3
	47.9	51.2	20.138	20.732	28.106	4.1799	0.9972	0.76	1.09	105.47
	48	51.2	20.148	20.742	28.613	4.1797	0.9971	0.764	1.09	105.56
	48	51.2	20.181	20.775	28.431	4.1798	0.9972	0.764	1.09	105.56
	47.9	51.2	20.174	20.768	28.213	4.1798	0.9972	0.755	1.1	105.85
	51.7	55.5	20.201	20.795	30.119	4.1795	0.9969	0.719	1.17	120.26
	51.4	55.2	20.228	20.822	29.598	4.1796	0.997	0.735	1.17	120.64
	51.5	55.3	20.222	20.816	29.506	4.1796	0.997	0.729	1.17	120.83
	51.8	55.6	20.222	20.816	30.099	4.1795	0.9969	0.71	1.17	120.93
	51.6	55.4	20.211	20.805	29.664	4.1796	0.997	0.725	1.17	121.03
	51.8	55.6	20.248	20.842	30.165	4.1795	0.9969	0.719	1.17	121.03
	51.4	55.2	20.254	20.848	29.834	4.1796	0.997	0.748	1.17	121.13
	51.9	55.7	20.227	20.82	30.189	4.1795	0.9969	0.704	1.17	121.61
								From the earlier test		30.4
										30.4
										30.5
										30.6
										30.4

A	X	Y	Z	AA	AB	AC	AD	AE	AF	AG	AH
1											
2			73	74	75	76	77	78	79		
3			Test 44	Test 44	Test 44	Test 44	Test 44	Test 44	Test 44		
4	Qin avg	Qin stdev	PM	Heat Flow out	Heat loss	% loss	Evap Avg	Cond Avg	Delta T	Delta T avg	Delta T stdev
77	45.828	0.187	0.146	37.593	8.502	18.44	35.473	33.784	1.689	1.8398	0.2315896
78	0	0	0.148	47.549	13.04	21.52	40.026	37.6	2.426	0	0
79	0	0	0.148	47.396	13.251	21.85	40.109	37.71	2.399	0	0
80	0	0	0.148	47.395	13.466	22.13	40.188	37.778	2.409	0	0
81	0	0	0.148	50.145	10.988	17.97	40.055	37.634	2.421	0	0
82	60.898	0.295	0.148	47.357	13.905	22.7	40.325	37.864	2.461	2.4232	0.0236051
83	0	0	0.149	59.218	16.146	21.42	44.528	41.241	3.287	0	0
84	0	0	0.15	60.116	15.471	20.47	44.646	41.373	3.273	0	0
85	0	0	0.149	58.045	17.766	23.43	44.529	41.285	3.244	0	0
86	0	0	0.149	56.21	19.76	26.01	44.583	41.328	3.255	0	0
87	75.786	0.3232	0.15	58.042	18.153	23.82	44.742	41.432	3.31	3.2738	0.0261094
88	0	0	0.152	70.678	19.813	21.89	48.886	44.757	4.129	0	0
89	0	0	0.151	73.036	17.542	19.37	48.958	44.85	4.109	0	0
90	0	0	0.151	69.492	21.086	23.28	48.84	44.71	4.13	0	0
91	0	0	0.152	72.341	18.324	20.21	49.049	44.881	4.168	0	0
92	90.613	0.0992	0.15	65.759	24.993	27.54	48.788	44.638	4.15	4.1372	0.02251
93	0	0	0.153	81.153	24.146	22.93	53.145	48.075	5.07	0	0
94	0	0	0.153	78.387	26.912	25.56	53.031	47.952	5.078	0	0
95	0	0	0.152	77.9	27.569	26.14	53.028	47.955	5.073	0	0
96	0	0	0.153	83.515	22.047	20.89	53.09	48.01	5.079	0	0
97	0	0	0.153	81.242	24.321	23.04	53.046	47.985	5.061	0	0
98	105.51	0.2051	0.151	78.1	27.745	26.21	53.006	47.958	5.049	5.06833	0.0114833
99	0	0	0.144	93.13	27.132	22.56	57.685	51.686	5.999	0	0
100	0	0	0.147	89.565	31.079	25.76	57.381	51.452	5.929	0	0
101	0	0	0.146	87.984	32.842	27.18	57.483	51.518	5.964	0	0
102	0	0	0.142	91.499	29.427	24.33	57.771	51.809	5.962	0	0
103	0	0	0.145	89.198	31.829	26.3	57.587	51.603	5.984	0	0
104	0	0	0.144	93.117	27.91	23.06	57.719	51.733	5.986	0	0
105	0	0	0.15	93.361	27.767	22.92	57.334	51.418	5.916	0	0
106	120.93	0.3901	0.141	91.596	30.017	24.68	57.854	51.852	6.002	5.96775	0.0315629
107											
108			0.148	24.1	6.3	20.72%	30.62	29.52	1.1		
109			0.148	24.2	6.2	20.39%	30.62	29.51	1.11		
110			0.147	24.3	6.2	20.33%	30.63	29.52	1.11		
111			0.147	25	5.6	18.30%	30.62	29.54	1.08		
112	30.46	0.08	0.147	25.4	5	16.45%	30.61	29.54	1.07	1.094	0.0063246

Appendix C: Uncertainty Calculations

Uncertainty calculations for ΔT :

$$\Delta T = \frac{tc3 + tc5}{2} - \frac{tc36 + tc37 + tc38}{2} \quad tc = \text{thermocouple}$$

$$d\Delta T = \left| \left(\frac{d}{d tc3} \Delta T \right) \cdot \delta tc3 \right| + \left| \left(\frac{d}{d tc5} \Delta T \right) \cdot \delta tc5 \right| + \left| \left(\frac{d}{d tc36} \Delta T \right) \cdot \delta tc36 \right| + \left| \left(\frac{d}{d tc37} \Delta T \right) \cdot \delta tc37 \right| + \left| \left(\frac{d}{d tc38} \Delta T \right) \cdot \delta tc38 \right| \dots$$

$$d\Delta T = \left| \frac{1}{2} \cdot \delta tc3 \right| + \left| \frac{1}{2} \cdot \delta tc5 \right| + \left| \frac{1}{3} \cdot \delta tc36 \right| + \left| \frac{1}{3} \cdot \delta tc37 \right| + \left| \frac{1}{3} \cdot \delta tc38 \right|$$

The estimate in the uncertainty for the thermocouple temperature measured using the Fluke data logger is, according to the Fluke specifications, $\pm 0.65 \text{ }^\circ\text{C}$. This is the uncertainty then for all thermocouple temperatures.

$$\delta tc3 = \delta tc5 = \delta tc36 = \delta tc37 = \delta tc38 = \delta tc$$

Thus we have: $d\Delta T = 2 \cdot \delta tc = 2 \cdot 0.65 \text{ }^\circ\text{C} = 1.3 \text{ }^\circ\text{C}$

$$\Delta T_{pt} = \text{Data_point} = \frac{\Delta T_1 + \Delta T_2 + \Delta T_3 + \dots + \Delta T_n}{n}$$

$$d\Delta T_{pt} = \left| \left(\frac{d}{d\Delta T_1} \Delta T_{pt} \right) \cdot \delta\Delta T_1 \right| + \left| \left(\frac{d}{d\Delta T_2} \Delta T_{pt} \right) \cdot \delta\Delta T_2 \right| + \dots + \left| \left(\frac{d}{d\Delta T_n} \Delta T_{pt} \right) \cdot \delta\Delta T_n \right|$$

$$\frac{d}{d\Delta T_1} \Delta T_{pt} = \frac{1}{n} \quad \dots \quad \frac{d}{d\Delta T_n} \Delta T_{pt} = \frac{1}{n}$$

$$d\Delta T_{pt} = \left| \frac{1}{n} \cdot \delta\Delta T_1 \right| + \left| \frac{1}{n} \cdot \delta\Delta T_2 \right| + \dots + \left| \frac{1}{n} \cdot \delta\Delta T_n \right| \quad \text{where } \delta\Delta T_n \text{ is given above as: } \delta\Delta T_n = 1.3 \text{ }^\circ\text{C}$$

$$d\Delta T_{pt} = \frac{1}{n} \cdot n \cdot \delta\Delta T_n = 1.3 \text{ }^\circ\text{C} \quad \text{So it doesn't matter how many data points are averaged, the uncertainty for a plotted point is constant at } \pm 1.3 \text{ }^\circ\text{C}.$$

Uncertainty calculations for Q_{in} :

$$\text{Power} = I^2 \cdot R = Q_{in} \quad R := 88.2 \cdot \text{ohm}$$

$$dQ_{in} = \left| \left(\frac{d}{dI} Q_{in} \right) \cdot \delta I \right| + \left| \left(\frac{d}{dR} Q_{in} \right) \cdot \delta R \right| = |2 \cdot I \cdot R \cdot \delta I| + |I^2 \cdot \delta R|$$

$$\frac{dQ_{in}}{Q_{in}} = \left| \frac{2 \cdot I \cdot R \cdot \delta I}{I^2 \cdot R} \right| + \left| \frac{I^2 \cdot \delta R}{I^2 \cdot R} \right| = \left| \frac{2 \cdot \delta I}{I} \right| + \left| \frac{\delta R}{R} \right|$$

The current is measured through a shunt resistor.

$$I = \frac{V}{R_{shunt}} \quad \delta I = \left| \left(\frac{d}{dV} I \right) \cdot \delta V \right| + \left| \left(\frac{d}{dR_{shunt}} I \right) \cdot \delta R_{shunt} \right| = \left| \frac{1}{R_{shunt}} \cdot \delta V \right| + \left| \frac{-V}{R_{shunt}^2} \cdot \delta R_{shunt} \right|$$

$$\frac{\delta I}{I} = \left| \frac{\frac{1}{R_{shunt}} \cdot \delta V}{\frac{V}{R_{shunt}}} \right| + \left| \frac{\frac{-V}{R_{shunt}^2} \cdot \delta R_{shunt}}{\frac{V}{R_{shunt}}} \right| = \left| \frac{\delta V}{V} \right| + \left| \frac{-\delta R_{shunt}}{R_{shunt}} \right|$$

$$R_{shunt} := 0.01 \cdot \text{ohm}$$

The shunt was known to be a precision resistor with 1% accuracy, $\delta R_{shunt} := 1\% \cdot R_{shunt}$ thus:

δV is found from the Fluke data acquisition system, the specifications for the millivolt range: $0.01\% + 40 \cdot \mu\text{V}$

The maximum voltage that would be read at the shunt for the currents expected is 15 mV (which corresponds to 1.5 amps).

$$\mu\text{V} := 1 \cdot 10^{-6} \cdot \text{volt}$$

$$V := 1 \cdot \text{volt}$$

$$\delta V := 15 \cdot \text{mV} \cdot 0.01\% + 40 \cdot \mu\text{V}$$

$$15 \cdot \text{mV} \cdot 0.01\% = 0.0015 \cdot \text{mV}$$

$$\delta V = 0.0415 \cdot \text{mV}$$

$$40 \cdot \mu\text{V} = 0.04 \cdot \text{mV}$$

To be conservative $\frac{\delta V}{V}$ will be estimated at the lowest expected voltage, that is for the 15 watt input.

At 15 watts the expected voltage is: $I^2 \cdot R = 15 \text{ watt}$ or $I = \frac{1}{\sqrt{R}} \cdot \sqrt{15 \cdot \sqrt{\text{watt}}}$

$$V_{\min} = I \cdot R_{\text{shunt}} \quad V_{\min} = 4.1239 \cdot \text{mV} \quad I = 0.4124 \cdot \text{amp}$$

$$\frac{\delta V}{V_{\min}} = 1.0063 \cdot \%$$

$$\frac{\delta I}{I} = \left| \frac{\delta V}{V_{\min}} \right| + \left| \frac{-\delta R_{\text{shunt}}}{R_{\text{shunt}}} \right| \quad \left| \frac{\delta V}{V_{\min}} \right| + \left| \frac{-\delta R_{\text{shunt}}}{R_{\text{shunt}}} \right| = 2.0063 \cdot \%$$

Now we can determine the uncertainty in Q_{in} : $\frac{dQ_{\text{in}}}{Q_{\text{in}}} = \left| \frac{2 \cdot \delta I}{I} \right| + \left| \frac{\delta R}{R} \right| = 2 \cdot 2.0063 \cdot \% + 1 \cdot \%$

$$2 \cdot 2.0063 \cdot \% + 1 \cdot \% = 5.0126 \cdot \%$$

So the uncertainty in Q_{in} is: $\frac{dQ_{\text{in}}}{Q_{\text{in}}} = 5.0126 \cdot \%$

Heat loss through insulation at evaporator:

Problem: Determine the heat loss from the loop heat pipe tests that flow through the

Assumptions: The flow will take place as a natural convection. The heat flow thru the insulation must balance that which is to the freestream by convection.

Solution: From Incropera and Dewitt's text on Heat transfer (1985, pages 391-401) we get the following Nusselt relations for free convection:

For horizontal surfaces:

$$\text{For upper surface of heated plate: } Nu_L = 0.54 \cdot Ra_L^{\frac{1}{4}} \quad 10^4 \leq Ra_L \leq 10^7$$

$$\text{For lower surface of heated plate: } Nu_L = 0.27 \cdot Ra_L^{\frac{1}{3}} \quad 10^5 \leq Ra_L \leq 10^{10}$$

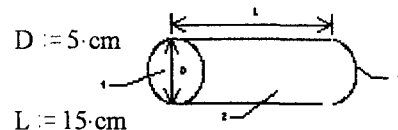
$$Ra_L = \frac{g \cdot \beta \cdot (T_s - T_{inf}) \cdot L^3}{\nu \cdot \alpha} \quad L = \frac{A_s}{P}$$

$$\text{For a long horizontal Cylinder: } Nu_D = \left[0.60 + \frac{0.387 \cdot Ra_D^{\frac{1}{6}}}{\left[1 + \left(\frac{0.559}{Pr} \right)^{\frac{9}{16}} \right]^{\frac{8}{27}}} \right]^2 \quad 10^{-5} \leq Ra_L \leq 10^{12}$$

For vertical surfaces:

$$Nu_L = \left[0.825 + \frac{0.387 \cdot Ra_L^{\frac{1}{6}}}{\left[1 + \left(\frac{0.492}{Pr} \right)^{\frac{9}{16}} \right]^{\frac{8}{27}}} \right]^2$$

The estimated dimensions of the cylinder used are:



To gain an appreciation for the magnitude of the effects of free convection on the heat loss through the insulation of the evaporator, two orientation will be evaluated; the evaporator vertical, the evaporator horizontal.

When the evaporator is vertical surfaces 1 and 3 will be considered horizontal surfaces (case 1). When the evaporator is horizontal surface 1 and 3 will be considered vertical surfaces and the sides considered as a cylinder (case 2).

Properties for air:

	T	ν	α	k	Pr
	(K)	$\left(\frac{\text{m}^2}{\text{sec}}\right)$	$\left(\frac{\text{m}^2}{\text{sec}}\right)$	$\left(\frac{\text{watt}}{\text{m}\cdot\text{K}}\right)$	
properties :=	250	$11.44 \cdot 10^{-6}$	$15.9 \cdot 10^{-6}$	$22.3 \cdot 10^{-3}$	0.720
	300	$15.89 \cdot 10^{-6}$	$22.5 \cdot 10^{-6}$	$26.3 \cdot 10^{-3}$	0.707
	350	$20.92 \cdot 10^{-6}$	$29.9 \cdot 10^{-6}$	$30.0 \cdot 10^{-3}$	0.700

$$g := 9.81 \cdot \frac{\text{m}}{\text{sec}^2}$$

For all testing the ambient temperature was never below 22.2 C $T_{\text{inf}} := (273.15 + 22.2) \cdot \text{K}$

The surface temperature at the outside of the insulation varies with the heat input to the evaporator but never exceeded 31.2 C:

$T_s := (273.15 + 31.2) \cdot \text{K}$	$i := 0..2$	$T_{\text{film}} := \frac{T_s + T_{\text{inf}}}{2}$	$\nu_{\text{values}_i} := \text{properties}_{i,1} \cdot \frac{\text{m}^2}{\text{sec}}$
$T_s - T_{\text{inf}} = 9 \cdot \text{K}$		$T_{\text{film}} = 299.85 \cdot \text{K}$	$T_{\text{values}_i} := \text{properties}_{i,0} \cdot \text{K}$
$\nu(T) := \text{linterp}(T_{\text{values}}, \nu_{\text{values}}, T)$		$\nu(T_{\text{film}}) = 1.588 \cdot 10^{-5} \cdot \frac{\text{m}^2}{\text{sec}}$	$\alpha_{\text{values}_i} := \text{properties}_{i,2} \cdot \frac{\text{m}^2}{\text{sec}}$
$\alpha(T) := \text{linterp}(T_{\text{values}}, \alpha_{\text{values}}, T)$		$\alpha(T_{\text{film}}) = 2.248 \cdot 10^{-5} \cdot \frac{\text{m}^2}{\text{sec}}$	$k_{\text{values}_i} := \text{properties}_{i,3} \cdot \frac{\text{watt}}{\text{m}\cdot\text{K}}$
$\beta(T) := \frac{1}{T}$		$\beta(T_{\text{film}}) = 0.003 \cdot \text{K}^{-1}$	$\text{Pr}_{\text{values}_i} := \text{properties}_{i,4}$
$k(T) := \text{linterp}(T_{\text{values}}, k_{\text{values}}, T)$		$k(T_{\text{film}}) = 0.026 \cdot \frac{\text{watt}}{\text{m}\cdot\text{K}}$	
$\text{Pr}(T) := \text{linterp}(T_{\text{values}}, \text{Pr}_{\text{values}}, T)$		$\text{Pr}(T_{\text{film}}) = 0.707$	

For evaporator in vertical position:

$$\text{Area}_{\text{sides}} := 2 \cdot \pi \cdot \frac{D}{2} \cdot L \quad \text{Area}_{\text{sides}} = 235.619 \cdot \text{cm}^2$$

$$\text{Ra}_L(T_s, T_{\text{inf}}) := \frac{g \beta \left(\frac{T_s + T_{\text{inf}}}{2} \right) \cdot \left[(T_s - T_{\text{inf}}) \cdot L^3 \right]}{\nu \left(\frac{T_s + T_{\text{inf}}}{2} \right) \cdot \alpha \left(\frac{T_s + T_{\text{inf}}}{2} \right)} \quad \text{Ra}_L(T_s, T_{\text{inf}}) = 2.784 \cdot 10^6$$

For vertical surfaces:

$$\text{Nu}_L(T_s, T_{\text{inf}}) := \left[0.825 + \frac{0.387 \cdot \text{Ra}_L(T_s, T_{\text{inf}})^{\frac{1}{6}}}{\left[1 + \left(\frac{0.492}{\text{Pr} \left(\frac{T_s + T_{\text{inf}}}{2} \right)} \right)^{\frac{9}{16}} \right]^{\frac{8}{27}}} \right]^2 \quad \text{Nu}_L(T_s, T_{\text{inf}}) = 21.825$$

$$\text{Nu} = \frac{h \cdot L}{k} \quad h(T_s, T_{\text{inf}}) = \frac{k \left(\frac{T_s + T_{\text{inf}}}{2} \right) \cdot \text{Nu}_L(T_s, T_{\text{inf}})}{L} \quad h(T_s, T_{\text{inf}}) = 3.825 \cdot \frac{\text{watt}}{\text{m}^2 \cdot \text{K}}$$

$$Q(T_s, T_{\text{inf}}) := \text{Area}_{\text{sides}} \cdot h(T_s, T_{\text{inf}}) \cdot (T_s - T_{\text{inf}})$$

$$Q(T_s, T_{\text{inf}}) = 0.811 \cdot \text{watt} \quad \text{This is the expected heat loss at the surface of the insulation for the sides only.}$$

For horizontal surfaces:

$$\text{Area}_{\text{ends}} := 2 \cdot \pi \cdot \left(\frac{D}{2} \right)^2$$

$$\text{For upper surface of heated plate: } \text{Nu}_L = 0.54 \cdot \text{Ra}_L^{\frac{1}{4}} \quad 10^4 \leq \text{Ra}_L \leq 10^7$$

$$\text{For lower surface of heated plate: } \text{Nu}_L = 0.27 \cdot \text{Ra}_L^{\frac{1}{3}} \quad 10^5 \leq \text{Ra}_L \leq 10^{10}$$

$$\text{Ra}_D(T_s, T_{\text{inf}}) := \frac{g \beta \left(\frac{T_s + T_{\text{inf}}}{2} \right) \cdot [(T_s - T_{\text{inf}}) \cdot D^3]}{\nu \left(\frac{T_s + T_{\text{inf}}}{2} \right) \cdot \alpha \left(\frac{T_s + T_{\text{inf}}}{2} \right)} \quad \text{Ra}_D(T_s, T_{\text{inf}}) = 1.031 \cdot 10^5$$

$$\text{Nu}_{\text{Lupper}}(T_s, T_{\text{inf}}) := 0.54 \cdot \text{Ra}_D(T_s, T_{\text{inf}})^{\frac{1}{4}}$$

$$\text{Nu}_{\text{Llower}}(T_s, T_{\text{inf}}) := 0.27 \cdot \text{Ra}_D(T_s, T_{\text{inf}})^{\frac{1}{3}}$$

$$\text{Nu} = \frac{h \cdot L}{k} \quad h_{\text{up}}(T_s, T_{\text{inf}}) := \frac{k \left(\frac{T_s + T_{\text{inf}}}{2} \right) \cdot \text{Nu}_{\text{Lupper}}(T_s, T_{\text{inf}})}{D} \quad h_{\text{up}}(T_s, T_{\text{inf}}) = 5.088 \cdot \frac{\text{watt}}{\text{m}^2 \cdot \text{K}}$$

$$h_{\text{low}}(T_s, T_{\text{inf}}) := \frac{k \left(\frac{T_s + T_{\text{inf}}}{2} \right) \cdot \text{Nu}_{\text{Lower}}(T_s, T_{\text{inf}})}{D} \quad h_{\text{low}}(T_s, T_{\text{inf}}) = 6.657 \cdot \frac{\text{watt}}{\text{m}^2 \cdot \text{K}}$$

$$Q_v(T_s, T_{\text{inf}}) := \text{Area}_{\text{ends}} \cdot (h_{\text{up}}(T_s, T_{\text{inf}}) + h_{\text{low}}(T_s, T_{\text{inf}})) \cdot (T_s - T_{\text{inf}})$$

$$Q_v(T_s, T_{\text{inf}}) = 0.415 \cdot \text{watt} \quad \text{This is the expected heat loss from the ends only.}$$

Total heat loss of evaporator through the insulation: $Q_v(T_s, T_{\text{inf}}) + Q(T_s, T_{\text{inf}}) = 1.226 \cdot \text{watt}$

Now for case 2, the evaporator horizontal:

$$\text{For a long horizontal Cylinder: } \text{Nu}_D(T_s, T_{\text{inf}}) := \left[0.60 + \frac{0.387 \cdot \text{Ra}_D(T_s, T_{\text{inf}})^{\frac{1}{6}}}{\left[1 + \left(\frac{0.559}{\text{Pr} \left(\frac{T_s + T_{\text{inf}}}{2} \right)} \right)^{\frac{9}{16}} \right]^{\frac{8}{27}}} \right]^2$$

for $10^{-5} \leq \text{Ra}_L \leq 10^{12}$

For vertical surfaces:

(note Ra_D is used since for the horizontal configuration the ends will be the vertical surfaces)

$$\text{Nu}_L(T_s, T_{\text{inf}}) := \left[0.825 + \frac{0.387 \cdot \text{Ra}_D(T_s, T_{\text{inf}})^{\frac{1}{6}}}{\left[1 + \left(\frac{0.492}{\text{Pr} \left(\frac{T_s + T_{\text{inf}}}{2} \right)} \right)^{\frac{9}{16}} \right]^{\frac{8}{27}}} \right]^2$$

$$\text{Ra}_D(T_s, T_{\text{inf}}) = 1.031 \cdot 10^5$$

$$\text{Nu} = \frac{h \cdot L}{k} \quad h_{\text{sides}}(T_s, T_{\text{inf}}) := \frac{k \left(\frac{T_s + T_{\text{inf}}}{2} \right) \cdot \text{Nu}_D(T_s, T_{\text{inf}})}{D} \quad h_{\text{sides}}(T_s, T_{\text{inf}}) = 4.12 \cdot \frac{\text{watt}}{\text{m}^2 \cdot \text{K}}$$

$$h_{\text{ends}}(T_s, T_{\text{inf}}) := \frac{k \left(\frac{T_s + T_{\text{inf}}}{2} \right) \cdot \text{Nu}_L(T_s, T_{\text{inf}})}{D} \quad h_{\text{ends}}(T_s, T_{\text{inf}}) = 4.878 \cdot \frac{\text{watt}}{\text{m}^2 \cdot \text{K}}$$

$$Q_s(T_s, T_{inf}) := \text{Area}_{sides} \cdot h_{sides}(T_s, T_{inf}) \cdot (T_s - T_{inf}) \quad Q_s(T_s, T_{inf}) = 0.874 \cdot \text{watt}$$

$$Q_e(T_s, T_{inf}) := \text{Area}_{ends} \cdot h_{ends}(T_s, T_{inf}) \cdot (T_s - T_{inf}) \quad Q_e(T_s, T_{inf}) = 0.172 \cdot \text{watt}$$

$$\text{Total heat loss for the horizontal configuration } Q_s(T_s, T_{inf}) + Q_e(T_s, T_{inf}) = 1.046 \cdot \text{watt}$$

So we see that the vertical configuration is the worst case configuration and it has less than a 1.23 watt heat loss at the evaporator. This then provides good confidence that the majority of the heat input to the evaporator does indeed enter the evaporator.

At a heat input of 75watts, 1.23 watts is 1.6% of the heat loss

Uncertainty calculations for Q_{out} :

Determining the error for the heat out at the condenser end.

$$Q_{out}(V_{dot}, c_p, \rho, \Delta T) := V_{dot} \cdot \rho \cdot c_p \cdot \Delta T \quad m_{dot} = V_{dot} \cdot \rho$$

$$dQ_{out}(V_{dot}, c_p, \rho, \Delta T, \delta V_{dot}, \delta c_p, \delta \rho, \delta \Delta T) := \left| \left(\frac{d}{dV_{dot}} V_{dot} \cdot \rho \cdot c_p \cdot \Delta T \right) \cdot \delta V_{dot} \right| \dots$$

$$+ \left| \left(\frac{d}{d\rho} V_{dot} \cdot \rho \cdot c_p \cdot \Delta T \right) \cdot \delta \rho \right| \dots$$

$$+ \left| \left(\frac{d}{dc_p} V_{dot} \cdot \rho \cdot c_p \cdot \Delta T \right) \cdot \delta c_p \right| \dots$$

$$+ \left| \left(\frac{d}{d\Delta T} V_{dot} \cdot \rho \cdot c_p \cdot \Delta T \right) \cdot \delta \Delta T \right|$$

$$V_{dot} := 0.15 \cdot \frac{\text{liter}}{\text{min}} \quad \rho := .99823 \cdot 10^3 \cdot \frac{\text{kg}}{\text{m}^3} \quad c_p := 4.1819 \cdot \frac{\text{kJ}}{\text{kg} \cdot \text{K}}$$

The flow rate was maintained between 0.1 liters/min and 0.2 liter/min for the majority of testing. For some tests it was higher, but typically did not exceed 0.4 liter/min.

$$\Delta T := 1.5 \cdot \text{K}$$

It was attempted to maintain the difference in temperature to at least 2 °C. For some of the low Q_{in} values this dropped to 1.5 °C.

For the flowmeter the specifications indicated an accuracy of 1% of the flow:

$$\delta V_{dot} := 1\% \cdot V_{dot}$$

The change in density and specific heat are estimated at 1%

$$\delta \rho := 1\% \cdot \rho \quad \delta c_p := 1\% \cdot c_p$$

From the Fluke the uncertainty in the temperature measurements is 1.3 C for a difference between temperatures

$$\delta \Delta T := 1.3 \cdot \text{K}$$

$$dQ_{out}(V_{dot}, c_p, \rho, \Delta T, \delta V_{dot}, \delta c_p, \delta \rho, \delta \Delta T) = 14.037 \cdot \text{watt} \quad V_{dot} \cdot \rho \cdot c_p \cdot \Delta T = 15.654 \cdot \text{watt}$$

As a percentage the uncertainty is calculated as:

$$dQ_{\text{out}}\%(\dot{V}_{\text{dot}}, c_p, \rho, \Delta T, \delta \dot{V}_{\text{dot}}, \delta c_p, \delta \rho, \delta \Delta T) := \frac{dQ_{\text{out}}(\dot{V}_{\text{dot}}, c_p, \rho, \Delta T, \delta \dot{V}_{\text{dot}}, \delta c_p, \delta \rho, \delta \Delta T)}{Q_{\text{out}}(\dot{V}_{\text{dot}}, c_p, \rho, \Delta T)}$$

For the given values above, which represent a conservative estimate the uncertainty as percentage is found to be:

$$dQ_{\text{out}}\%(\dot{V}_{\text{dot}}, c_p, \rho, \Delta T, \delta \dot{V}_{\text{dot}}, \delta c_p, \delta \rho, \delta \Delta T) = 89.7\%$$

Appendix D: Test Matrix

Test #	ΔH (meters)	Coolant Temperature (°C)	Evaporator Angle (degrees)	Condenser Angle (degrees)
3	0	20	0	0
4	0	20	45	0
5	0	20	135	0
6	0	20	90	0
7	0	20	0	45
8	0	20	0	90
9	0	20	0	-45
10	0	20	0	-90
11	0	40	0	-90
12	0	40	0	0
13	0	40	45	0
14	0	40	90	0
15	0	40	135	0
16	0	40	-45	0
17	0	40	-90	0
18	0	40	0	45
19	0	40	0	90
20	0	40	0	-45
21	0	20	-45	0
22	0	20	-90	0
23	0.61	20	0	0
24	1.22	20	0	0
25	1.83	20	0	0
26	2.44	20	0	0
27	2.79	20	0	0
28	0.61	20	0	0
29	1.22	20	0	0
30	1.83	20	0	0

Test #	ΔH (meters)	Coolant Temperature (°C)	Evaporator Angle (degrees)	Condenser Angle (degrees)
31	2.44	20	0	0
32	2.79	20	0	0
33	2.44	20	45	0
34	2.44	20	90	0
35	2.44	20	-45	0
36	2.44	20	-90	0
37	2.44	20	0	45
38	2.44	20	0	90
39	2.44	20	0	-45
40	2.44	20	0	-90
41	1.22	20	0	-90
42	1.22	20	0	-45
43	1.22	20	0	45
44	1.22	20	0	90
45	1.22	20	45	0
46	1.22	20	90	0
47	1.22	20	-45	0
48	1.22	20	-90	0

Bibliography

Beam, Jerry, Director Thermal Laboratory WL/POOS-3, Wright Laboratory WPAFB OH.

Personal interview. February 1994.

Dickey, J.T. and G.P. Peterson. "Experimental and Analytical Investigation of a Capillary

Pumped Loop," Journal of Thermophysics and Heat Transfer. Vol. 8, No. 3:

602-607, July-Sept. 1994.

Gernert, Nelson J. and Richard L. Weidner. Improved Flexible Heat Pipe Cold Plate Final

Report, April 1993 to November 1993. Contract F33615-93-C-2324. Lancaster PA:

Thermacore, Inc., 21 February 1994

Incropera, Frank P. and David P. Dewitt. Introduction to Heat Transfer. New York:

John Wiley & Sons, 1985.

Maidanik, Yu. F., Yu G. Fershtater, K. A. Goncharov. "Capillary-Pump Loop for the

Systems of Thermal Regulation of Spacecraft," Proceedings of the 4th European

Symposium on Space Environmental and Control Systems, held in Florence, Italy,

2-24 October, 1991 (ESA SP-324, December 1991)

Maidanik, Jury F., Sergei V. Vershinin, Valery F. Kholodov, Jury D. Dolgirev. Heat

Transfer Apparatus. United States Patent number 4,515,209. May 7, 1985

Meyer, Rudiger, Robert Muller, Klaus Beckman, K. A. Goncharov, E. Yu Kotlyarov, Yu F. Maidanik. "Investigation of the Heat Transfer Performance of a Capillary Pumped Ammonia Loop Under Gravity," 23rd International Conference on Environmental Systems, Colorado Springs CO. July 12-15, 1993. SAE Technical Paper Series 932304.

Russian Loop Heat Pipe. Data sheets from preliminary testing provided with the purchase of the loop heat pipe. Provided to Wright Laboratories, WL/POOS. July, 7 1992.

Vita

Captain Brad R. Thompson was born on March 17th, 1960 in Bremerton, Washington. His early years were spent in Marysville, Washington and Edmonds Washington, where he graduated from Edmonds High School in 1978. He enlisted in the Air Force in September 1979, and for the next 8 years served as an Aircraft Loadmaster on both the C-130 and C-5 aircraft. In 1987, then Staff Sergeant Thompson was accepted to the Airman Education and Commissioning Program and assigned to Arizona State University in Tempe, Arizona. He graduated Magna Cum Laude in May of 1990, earning a Bachelor of Science in Mechanical Engineering. Following Officer Training School, his first duty assignment was to the Advanced Cruise Missile System Program Office at Wright-Patterson Air Force Base, Ohio. While assigned to this organization, he served as Program Manager for the thirty-three million dollar Avionics Integration Support Facility, a highly complex depot capability for organically maintaining the Advanced Cruise Missile air vehicle and automatic test equipment software. He also managed the Advanced Cruise Missile Image Radar System, a program designed to ensure that the stealth characteristics of the missile are preserved for the life of the missile. He entered the Air Force Institute of Technology to pursue a Master's Degree in Astronautical Engineering in May of 1993.

Permanent Address: 317-89th Street S.E.
Everett, Washington 98208

REPORT DOCUMENTATION PAGE

Form Approved
OMB No. 0704-0188

Public reporting burden for this collection of information is estimated to average 1 hour per response, including the time for reviewing instructions, searching existing data sources, gathering and maintaining the data needed, and completing and reviewing the collection of information. Send comments regarding this burden estimate or any other aspect of this collection of information, including suggestions for reducing this burden, to Washington Headquarters Services, Directorate for Information Operations and Reports, 1215 Jefferson Davis Highway, Suite 1204, Arlington, VA 22202-4302, and to the Office of Management and Budget, Paperwork Reduction Project (0704-0188), Washington, DC 20503.

1. AGENCY USE ONLY (Leave blank)		2. REPORT DATE December 1994	3. REPORT TYPE AND DATES COVERED Master's Thesis	
4. TITLE AND SUBTITLE EXPERIMENTAL INVESTIGATION OF THE EFFECTS OF RELATIVE PHYSICAL ORIENTATION BETWEEN EVAPORATOR AND CONDENSER FOR A LOOP HEAT PIPE			5. FUNDING NUMBERS	
6. AUTHOR(S) Brad R. Thompson, Capt, USAF				
7. PERFORMING ORGANIZATION NAME(S) AND ADDRESS(ES) AFIT/ENY 2950 P Street WPAFB OH 45433-7765			8. PERFORMING ORGANIZATION REPORT NUMBER AFIT/GA/ENY/94D-10	
9. SPONSORING/MONITORING AGENCY NAME(S) AND ADDRESS(ES) Dr. Jerry Beam WL/POOS 1950 5th Street			10. SPONSORING/MONITORING AGENCY REPORT NUMBER	
11. SUPPLEMENTARY NOTES				
12a. DISTRIBUTION/AVAILABILITY STATEMENT Approved for public release; distribution unlimited			12b. DISTRIBUTION CODE	
13. ABSTRACT (Maximum 200 words) This research examined the effects on performance of varying angular orientation and height differences between evaporator and condenser for a loop heat pipe. Performance was defined as the difference in temperature between evaporator and condenser (ΔT). The pipe was evaluated at varying input power (Q_{in}) for: varying evaporator and condenser angles, different coolant temperatures, and varying relative height differences. All analysis included only steady state operation. The performance was influenced by condenser angles, with an optimal condenser angle for best performance being +45 degrees from horizontal. Additionally, the evaporator angles were found to influence performance only at low Q_{in} and low coolant temperatures. For high Q_{in} , performance was independent of evaporator angle. For small Q_{in} the ΔT increased (poorer performance) with decreasing coolant temperature. However, for high Q_{in} the ΔT was independent of coolant temperature. For small Q_{in} , the ΔT increased with increasing heights of evaporator over condenser. However, for high Q_{in} the ΔT was independent of the height difference. Additionally, pipe operation was sensitive to the rate of decrease of Q_{in} . Finally, an unexplained anomaly shows the pipe to operate at two different ΔT values for a given heat input.				
14. SUBJECT TERMS Loop Heat Pipe (LHP), Capillary Pumped Loop (CPL), Heat Pipe			15. NUMBER OF PAGES 81	
			16. PRICE CODE	
17. SECURITY CLASSIFICATION OF REPORT Unclassified	18. SECURITY CLASSIFICATION OF THIS PAGE Unclassified	19. SECURITY CLASSIFICATION OF ABSTRACT Unclassified	20. LIMITATION OF ABSTRACT UL	